AFML–TR–71–264

IMPROVED FRACTURE TOUGHNESS OF Ti-6A1-4V THROUGH CONTROLLED DIFFUSION BONDING

D. COX
A.S. TETELMAN

FAILURE ANALYSIS ASSOCIATES

TECHNICAL REPORT AFML–TR–71–264

FEBRUARY 1972

AIR FORCE MATERIALS LABORATORY
AIR FORCE SYSTEMS COMMAND
WRIGHT-PATTERSON AIR FORCE BASE, OHIO

NOTICE

When Government drawings, specifications, or other data are used for any purpose other than in connection with a definitely related Government procurement operation, the United States Government thereby incurs no responsibility nor any obligation whatsoever; and the fact that the government may have formulated, furnished, or in any way supplied the said drawings, specifications, or other data, is not to be regarded by implication or otherwise as in any manner licensing the holder or any other person or corporation, or conveying any rights or permission to manufacture, use, or sell any patented invention that may in any way be related thereto.

Copies of this report should not be returned unless return is required by security considerations, contractual obligations, or notice on a specific document.

IMPROVED FRACTURE TOUGHNESS OF Ti-6Al-4V THROUGH CONTROLLED DIFFUSION BONDING

by

D. Cox
A. S. Tetelman
FAILURE ANALYSIS ASSOCIATES

TECHNICAL REPORT AFML-TR-71-264

February, 1972

AIR FORCE MATERIALS LABORATORY
AIR FORCE SYSTEMS COMMAND
WRIGHT-PATTERSON AIR FORCE BASE, OHIO

FOREWORD

This report was prepared by Failure Analysis Associates, Stanford, California. The work was performed under USAF Contract No. F33615-71-C-1062. The contract was initiated under Project No. 7381, "Materials Applications," Task No. 738106, "Design Information Development," and administered by the Air Force Materials Laboratory, Wright-Patterson Air Force Base, Ohio, Mr. C.L. Harmsworth (LAE), Project Engineer.

The authors wish to acknowledge Dr. Howard Hamilton of the Los Angeles Division of North American Rockwell Corp., who supervised fabrication of the billets for his excellent assistance, and UCLA for providing the facilities for testing the material.

This report covers work conducted from November 1970 to November 1971. The contract was monitored by Mr. C. L. Harmsworth/LAE.

The report was submitted by the authors in February 1972.

This technical report has been reviewed and is approved.

A. OLEVITCH
Chief, Materials Engineering Branch
Materials Support Division
Air Force Materials Laboratory

ABSTRACT

The use of laminate composites containing a weak interface to increase the fracture toughness of high strength titanium alloys has been studied. Billets were fabricated from .040 inch Ti-6Al-4V sheet material using a diffusion bonding process. Six billets were fabricated, each billet having an interface with different properties.

Weak interfaces were produced by incomplete diffusion bonding (two billets), by the use of a commercially pure titanium interleaf (two billets), or by the use of an unalloyed aluminum interleaf. One billet was fabricated with a full strength bond (no interleaf) for use as a control billet for comparison purposes.

Tensile tests on as-fabricated material were made to determine the interface bond strength. Fracture toughness tests were made using precracked Charpy specimens for material in both heat treated and annealed conditions. Three possible orientations of the crack to the interface were tested.

Results indicate that toughness, as measured by the precracked Charpy test, is increased when delamination or splitting of the bond occur. In the arrester orientation the toughness became very high as gross yielding occurred after delmaination. In the divider orientation the fracture mode was changed from plane strain to plane stress when delamination occurred and the fracture toughness for the composite approached the toughness of the .040 inch sheet used in fabrication. Decreases in

toughness occurred when the crack propagated along the bond plane. These results indicate that controlled diffusion bonding may offer promise for improving the toughness in certain directions of orthotropic metal laminates without producing significant decreases in transverse strength or toughness.

A simple model to predict the conditions necessary for delamination has been formulated. Correlations between the model and experimental results are made. The model can account for the effect of different base metal and interface material properties and thicknesses. It is seen that a thin, low yield strength interface material with a full strength diffusion bond to a high yield strength, fairly tough base metal leads to optimum composite toughness.

TABLE OF CONTENTS

LIST OF ILLUSTRATIONS

LIST OF ILLUSTRATIONS--continued

LIST OF LUSTRATIONS--continued

LIST OF TABLES

SECTION I

INTRODUCTION

There is a great need to develop high yield strength materials with high toughness. One traditional method of obtaining high toughness is through microstructural control or alloying. Another method is through the use of sub-macro laminated structures. By using a high strength alloy with alternating layers of a weaker interfacial material, a practical "composite" material which could give superior fracture behavior may be obtained. This report presents the results of work done in evaluating the mechanical properties of 6Al-4V titanium multi-laminate materials for possible application to Air Force systems.

The use of a laminate structure to increase toughness is based upon the relaxation of triaxial constraint which is developed ahead of the crack tip. If the interface is sufficiently weak, the triaxial stresses or strains will cause delamination or separations ahead of the crack. This causes a moving crack to blunt out (arrester orientation, Fig. 1) or causes the material to delaminate into tough thin sheets (divider orientation, Fig. 1).

There are basically three possible orientations of the interface in relation to a propagating crack (Fig. 1). In the arrester orientation the delamination would effectively blunt the crack. Gross yielding of the material follows; linear elastic fracture toughness criteria are then not applicable.

In the divider orientation, this delamination would cause the material to fail in the "plane stress" mode and toughness would again be increased. This results from the fact that the fracture toughness of thin sheets, K_c, is much greater than the plane strain fracture toughness, K_{Ic} (Fig. 2),

unless the sheets are very thin. However, if the crack lies in the weak interface plane, (enhancer orientation, Fig. 1), the fracture toughness may be lower. Even in uncracked material, the transverse strength of a macrolaminated composite will be somewhat less than that of the base material alone. The key question is whether increased longitudinal toughness through crack arrest and crack division can be achieved without severe loss in transverse strength, for a given application. Optimization of the laminate and interface characteristics will allow for increases in toughness in the arrester and divider cases without significant loss of load carrying capabilities in the direction perpendicular to the plane of the interface (enhancer geometry).

The superior fracture characteristics of laminated structures have been well documented.[1] Kaufman[2] working with 7075-T6 aluminum, showed that the K_c fracture toughness values of adhesively bonded laminates with the crack divider geometry were increased over those values for plate of the same overall thickness. Birkbeck et al.[3] made a comparison of multilayered (crack arrester) and solid wall steel shells of the same thickness. It was found that the ductile-brittle transition temperature was reduced when the layers were less than .25 inches thick. In this experimentation there was no bonding of any sort; the concentric shells were machined to fit with close tolerance. Leighter[4] found for a 5Al-2.5Sn titanium alloy that the K_c values could be increased up to seven times using crack divider geometry bonded with a silver braze alloy instead of plate of the same over-all thickness. It was also found in the crack arrester geometry that gross yielding must occur in the laminae before crack propagation can take place, and therefore high fracture toughness was achieved.

In order to determine the importance of bond strength in laminated materials, a number of bonding agents, methods, and strengths have been used. The bond strength must be sufficiently weak to allow delamination and relaxation of the triaxial constraint. Thus it was found that a metallurgically bonded panel of 7075-T6 did not show any advantage over a plate of the same thickness if the bond did not allow the formation of shear surface on the individual layers in the crack divider geometry.[2]

The transition temperature of a mild steel was reduced 80°C for the crack arrester geometry with a soft solder interface while it was reduced 140°C when an explosive bonded copper interface was used.[5] From these results it is apparent that the properties of the bond can also affect the behavior of the laminate.

McCartney et al.[6] have also examined the effect of different bond strengths on the fracture resistance of high strength steel. They considered the "interface-fracture strength gradient" or the rate of change of strength across the interface. A nickel interleaf was used to provide the weak bond. Delamination was enhanced when a steep nickel concentration gradient was present across the bond line. If the nickel concentration gradient was lowered by diffusion, it was found that delamination would not take place. From the results of their work they determined that the parameters which govern the crack arrest in the arrester geometry are the interfacial-fracture strength gradient and the plastic zone size of the propagating crack.

SECTION II

PURPOSE OF PRESENT STUDY

Previous studies discussed above indicate that increased toughness in the arrester and divider orientations is possible when a weak interface is present between layers of high strength base material. The present work was designed to determine quantitatively the degree of "weakening" that is required in the interface in order to achieve high toughness in the two other orientations. The studies were conducted to determine whether there is a potential for using this approach to improve toughness in high strength titanium alloys.

SECTION III

MATERIALS AND FABRICATION

The material selected for the study was 6Al-4V titanium mill annealed sheet (AMS 4911) .040 inches in thickness. This thickness was chosen so that a representative number of sheets (ten) would be present in the small (0.4" square), inexpensive Charpy specimens used in the work. Material from four different heats was used. During fabrication of the billets the sheets from different heats were alternated--1, 2, 3, 4, etc. The physical properties and chemical analysis for the four heats are shown in Tables I and II, respectively.

Three billets were fabricated using a metal foil as an interleaf material. Two of these used a 75A grade commercially pure titanium foil which was obtained in the annealed condition (AMS 4901). Of these one had a foil .005 inches in thickness while the second billet used a .010 inch commercially pure foil. The physical properties and chemical analysis of these foils are given in Tables III and IV. The third billet had a commercially pure aluminum foil .0015 inches in thickness as an interleaf material (1100 alloy). This was a typical heavy duty household foil and no mechanical testing or chemical analysis was made on the material.

All billets were fabricated using a diffusion bonding process. The actual bonding was done under sub-contract at North American Rockwell under the supervision of Dr. Howard Hamilton. The titanium sheet, retort, and tooling were prepared using established cleaning procedures. All diffusion bonding was conducted under vacuum of less than 10^{-4} torr. A heavy retaining ring, or yoke, was used to assure side restraint and prevent excess lateral deformation. Time, temperature, and pressure

depended upon bond strength desired or interleaf material used. The parameters used for each of the billets are shown in Table 5.

Six billets were fabricated. The as-fabricated tensile strength of the interface for the different billets is also shown in Table V. Billet size was nominally 7 inches wide by 7 inches long by 2.4 inches thick. Billet #1 was fabricated using the best established techniques to provide basic fracture behavior for comparison with the controlled bond strength billets. A UTS of 135 ksi perpendicular to the bond line was obtained. Figure 3 shows the typical microstructure of Billet #1. There is no evidence of microvoids. Billet #2 was fabricated with a controlled porosity bond of 68 ksi UTS perpendicular to the bond line. In Figure 4 the microstructure of this billet is shown and the remaining microvoids at the bond are easily visable. Billet #3 had a .005 inch commerically pure titanium foil interleaf between the lamella. The diffusion bonding process was such that a full strength bond was obtained and the UTS of this interleaf was 132 ksi. The microstructure of Billet #3 is shown in Figure 5.

Billet #4 was to have a controlled porosity bond with a UTS of 110 ksi. After fabrication, tensile tests indicated that the strength of the bond was only 75 ksi. It was decided that a diffusion heat treatment with no external pressure applied would be used to raise the bond strength to the desired level. A series of tensile specimen blanks were cut and treated at 1650°F for various times. The results of this series are shown in Table VI. From this work a treatment of 30 minutes at 1600°F was used on the actual Charpy specimen blanks. Tensile tests on material treated in this manner showed the resulting bond strength to be 142 ksi.

Figure 6a shows the microstructure and microvoids present in the as-fabricated billet while Figure 6b shows the same material after a thermal treatment of four hours at 1650°F.

Billet #5 incorporated in a commercially pure titanium foil. The foil thickness was .010 inches and the resulting interface UTS was 125 ksi. Billet #6 was fabricated using a .0015 inch aluminum interleaf. Tests showed the resulting interleaf to have a UTS of 38 ksi. Figure 7 shows the microstructure of this material and interface.

SECTION IV

TESTING PROCEDURES

Tensile tests on the as-fabricated billets were made by North American Rockwell. A round specimen .25 inches in diameter with a one inch gauge length was used in this testing and is shown in Figure 8. Two specimens from each billet were tested using a Baldwin testing machine and a strain rate of .005 in./in. minute. The complete results of the NAR tensile tests are shown in Table VII. The yield strength was calculated from the load at a strain of .002 in./in. Data was not obtained on Billet #1 since the fabrication process assured a full strength bond. Additional tensile data on the first four billets including Billet #1 were obtained by AFML. The specimen used is shown in Figure 9 and the results in Table VIII. The results are similar to the NAR results except for Billet #2 with the microvoid bond. This is probably due to the inherent nonuniformity of this type of bond which will be discussed in a later section.

Because of the limited nature of the program, it was desirable to use a relatively small, inexpensive specimen for the determination of fracture toughness. Therefore, precracked Charpy specimens (Fig. 10) were used in this study. Although such a specimen does not meet ASTM specimen criteria and the results are not considered valid K_{Ic} values, the values are considered valid in comparing the relative toughness characteristics of the materials evaluated. From each billet eighteen specimen blanks were machined--six from each of the three orientations shown in Figure 1. The rough specimens were then heat treated prior to final machining.

Three material conditions were used in this study. Except for specimens from Billet #6, half of the specimens were given an annealing heat treatment while the remaining half were solution treated and aged. The annealing treatment was conducted at UCLA and consisted of 1-1/2 hours at 1400°F in an NRC vacuum furnace followed by furnace cooling. The vacuum present during this treatment was better than 10^{-4} torr. Solution treatment of the remaining specimens was carried out in a Lindberg muffle furnace. The specimens were heated to 1600°F for twenty minutes in air. They were then water quenched. Aging was carried out in a Pacific muffle furnace. The specimens were placed in an O-ring sealed quartz tube and connected to a Duo Seal vacuum pump by a rubber hose. The treatment consisted of aging six hours at 950°F while the roughing pump maintained a vacuum of approximately 1.0 torr, to halt the possibility of further oxidation. The tube was then removed from the furnace and the specimens were allowed to air cool.

Since both the annealing and solution heat treatments involve temperatures above the melting point of aluminum, it was not possible to heat treat Billet #6 material to these conditions. Specimens from this billet were machined from the as-fabricated material. Since the alloy used for fabrication was in the mill annealed condition, these specimens would be in an annealed condition, although the final anneal was not made.

Final machining of the specimens was done after heat treatment to insure the removal of the surface oxidation which occurred during the heat treatment. After final machining the specimens were precracked using a Krouse fatigue machine. Precracking was done in three point bending. Approximately 50,000 cycles were used to obtain a fatigue crack of about .040 to .060 inches in depth.

The fracture toughness testing of the precracked Charpy specimens was carried out on an Instron tensile testing machine. The three point bend jig used is shown in Figure 11. The tests were run at room temperature and with a cross heat speed of 0.1 in./min. Three specimens for each of the three possible crack orientations for both heat treat conditions were tested for a total of eighteen specimens per billet, except for Billet #6 where only nine specimens were tested.

The fracture toughness values were obtained in the following manner. For the Charpy specimen used in this study it has been shown[7] that the crack tip stress intensity factor, K_I, is given by

$$K_I = Y \frac{6M}{W^3} \sqrt{a} \tag{1}$$

The applied moment, M, is given by

$$M = \frac{PL}{2} \tag{2}$$

where P is the applied load and L is the loading span. Thus

$$K_I = Y \frac{3PL}{W^3} \sqrt{a} \tag{3}$$

where W is the specimen width, a is the total crack depth and Y is the K calibration. A curve showing the K calibration for the Charpy specimen as a function of a/W has been calculated by Gross and Srawley.[7] Using this curve, the specimen dimensions, and the maximum applied load as determined from the load deflection curve, the fracture toughness was obtained.

Additional as-fabricated material from Billets 1, 2, 3, and 4 was sent to the AFML for fracture evaluation. After the material was annealed

tests were conducted using an ASTM recommended compact tension configuration as shown in Figure 27. Both precracking and fracture testing were conducted in accordance with ASTM E 399 criteria. A limited number of fatigue tests were also conducted at AFML on a 2 ton Schenck fatigue machine at a maximum stress level of 65 ksi and a stress ratio of R = 0.1. This specimen configuration is shown in Figure 29.

SECTION V

EFFECTS OF THERMAL TREATMENT ON TENSILE PROPERTIES

The tensile testing used to determine the interface bond strength was made on as-fabricated material before heat treating to the two conditions used in the fracture testing. From the work done on Billet #4 (Table VI) it is apparent that elevated temperatures for even relatively short times have a significant effect on the tensile properties of an interface containing microvoids. This can be explained by the faster rate of vacancy diffusion which occurs at these elevated temperatures. Figure 6 shows this effect on the microvoids which are present in the bond line. From the increase in bond strength (75 ksi to 142 ksi) which occurred with the final parameters used, it is apparent that this effect is drastic. Since both annealing and solution treatments involve high temperatures, the actual bond strength of the tested material which has a microviod interface will be higher, possibly very much higher than the as-fabricated material used in the tensile testing. Since tensile tests were not made on material from any of the billets after final annealing or heat treatment, the extent of this effect is unknown.

In Billets 1, 3, 5, and 6, the diffusion bond is full strength and the effect of the heat treatments will not be as significant. Inter-diffusion of alloy elements and impurities into the commercially pure titanium foil might increase the tensile strength of the foil slightly. However, the large increase in tensile strength of the joint over that of the foil material (approx. 99 ksi) is due to the constraint imposed by the surrounding Ti-6Al-4V material. The foil behaves similar to the braze material in a braized joint.[8] The aluminum interleaf would behave similarly. There is the possibility of the formation of an

intermetallic compound but with the temperature and time used in fabrication it is unlikely that it occurred. The micrograph shown in Figure 7 substantiates that no intermetallic has formed.

SECTION VI

RESULTS OF FRACTURE STUDIES

A summary of the fracture toughness results is shown in Table IX. Where delamination occurred in the arrester geometry, gross yielding and crack blunting followed and the fracture toughness could not be determined.

Billet #1 was used as a control for comparison with the other billets containing the various interfaces. The variation in toughness with orientation in Billet #1 is due to the anisotropic nature of the sheet material used in the fabrication.[9] Typical fracture appearances for the three orientations are shown in Figure 12.

Delamination in the arrester geometry occurred in both annealed and heat treated material of Billet #2. Photographs of these cases are shown in Figure 13. Shearing of the interface can also be seen, and was especially prevalent in the heat treated material.

Delamination and splitting also occurred in the divider geometry (Fig. 14) although the toughness was not increased for the annealed material with this orientation. The fracture surface of the enhancer orientation was very flat as can be seen in Figure 15.

Delamination in arrester orientation of Billet #3 only occurred in the heat treated material, Figure 16. The divider orientation did not split in the annealed condition and the fracture surface was not completely shear lip in the heat treated specimens (Fig. 17). Again the surface of the enhancer geometry was very flat (Fig. 18).

One annealed arrester specimen delaminated for Billet #4 while all three heat treated specimens with this orientation delaminated (Fig. 19). The divider behavior was similar to Billet #3. Little shear lip was

observed in the annealed material while the fracture surface of the heat treated material was virtually 100% shear (Fig. 20). Again, the enhancer fracture surface was flat and the crack propagated through the interface (Fig. 21).

No delamination occurred in Billet #5 and typical fracture surface appearances are shown in Figures 22, 23, and 24. Billet #6 was tested only in the as-fabricated (annealed) condition. Delamination and splitting occurred in both arrester and divider orientation in this billet (Figs. 25 and 26). The enhancer fracture surface was flat and fracture occurred through the foil interleaf (Fig. 26).

Fracture toughness testing, using ASTM recommended compact tension specimens (Fig. 27), was conducted by AFML on annealed material from the first four billets. These data are shown in Table X. The values are consistantly lower than those obtained from the precracked Charpy specimens. Figure 28 shows the fracture appearance of the AFML tests. As can be seen in Figure 28b and 28d, shearing of the interface in the arrester orientation occurred in Billets #2 and #4 and results were not obtained. Delamination or splitting also took place in these billets for the divider orientation. Fatigue tests at a single stress level were also performed on specimens from Billets #1-4. The results of these tests are shown in Table XI. There is a decrease in the fatigue strength when the loading is perpendicular to the interface.

Figures 30 and 31 show values of fracture toughness as a function of the relative bond strength for the two conditions tested. The relative bond strength was found by taking the ratio of the bond strengths for the billets to the bond strength for Billet #1. The NAR tensile data is

used with an assumed bond strength for Billet #1 of 145 ksi. Fracture toughness values used are those obtained from the precracked Charpy specimens.

Figure 30 shows that in the annealed condition with arrester geometry there is a general increase in fracture toughness with decrease in bond strength. The divider orientation shows a decrease in toughness in the weaker bonds. The general trend in the enhancer geometry is towards a decrease in fracture toughness with decrease in bond strength

In the heat treated material, delamination occurred in the arrester geometry for all specimens except those with the thicker titanium foil interleaf (Billet #5). There was little change in toughness with bond strength for the divider orientation. Again in the enhancer orientation there was a decrease in the fracture toughness with decrease in bond strength.

SECTION VII

THEORETICAL CONSIDERATIONS

In order to achieve an increase in toughness in these laminate materials, delamination ahead of the propagating crack must occur. Figure 32 shows the steps which lead to delamination and splitting of the interface in the arrester orientation. Triaxial constraint ahead of the crack tip produces transverse stress σ_{xx} and σ_{zz} in this region (Fig. 32a). In the arrester orientation the transverse σ_{xx} acts as a tensile stress across the interface. As discussed by Saxton et al.[8] this tensile stress produces a shear stress along the bond line which in turn produces a second hydrostatic stress field in the interface material. This secondary hydrostatic stress field reinforces the effect of the transverse stresses caused by the crack itself. This combined triaxial stress state produces localized yielding around void-nuclei present in the interface material (Fig. 32b). Fracture occurs at the interface ahead of the advancing crack by the growth and coalescence of the voids (Fig. 32c). The primary crack propagates to the delamination where it is effectively blunted (Fig. 32d). Further crack propagation requires extensive gross yielding.

The situation is similar in the divider orientation (Fig. 33). In this case the principle transverse stress which leads to splitting is the σ_{zz} stress ahead of the crack tip. The splitting of the interface causes the laminates to behave as the sum of many thin sheets. In this case, the fracture toughness approaches the plane stress toughness K_c. Since K_c can be a factor of 2 or 3 greater than K_{Ic} in high yield strength materials, delamination in the divider orientation can lead to a substantial increase in toughness.

The splitting of the interleaf type interface takes place in the interleaf by void formation and coalescence. In the microvoid interface, splitting takes place at the bond line by coalescence of the microvoids which are already present. This is seen in Figure 34 which shows a typical delamination surface for the divider orientation. The surface appearance is dimpled indicating a ductile type fracture.

From linear elastic fracture mechanics it is known that crack propagation under plane strain tensile loading will occur when the stress intensity factor of the crack, K_I, equals the fracture toughness of the material K_{Ic}. The stress intensity factor is of the form

$$K_I = \sigma \sqrt{\pi a \alpha} \qquad (4)$$

where σ is the applied stress, a is the crack length, and α is a parameter which depends upon the geometry of crack and specimen.[10] Thus for fast fracture at a stress $\sigma = \sigma_F$

$$K_{Ic} = \sigma_F \sqrt{\pi a \alpha} \qquad (5)$$

Therefore to achieve an increase in toughness by use of laminate composites, delamination and splitting must occur before the stress intensity factor equals the fracture toughness K_{Ic} of the material.

Ductile fracture of a material occurs when the plastic strain reaches some critical strain, ε_f. This criterion would apply for laminate composites where the interface failure has been shown to be dimple rupture (Fig. 34). Thus for delamination to occur, the local strain in the interface must reach some critical value, ε_f, before $K_I = K_{Ic}$.

McClintock has shown that this critical fracture strain is inversely proportional to the degree of triaxiality in the material.[11] West et al.[12] studied the fracture of thin braze joints under uniaxial loading (isostress conditions). It was found that during loading, constraint of the interface produces a triaxial stress state in the joint material. This hydrostatic stress state was found to be a function of joint thickness, increasing as the thickness was decreased.

Laminate materials behave similarly. Consider the divider orientation, where the transverse stress σ_{zz} is set up across the lamella and a triaxial stress state is formed at the base metal/lamella interface. This high degree of combined triaxiality will decrease the critical strain necessary for fracture in accordance with the McClintock model, which predicts a strong inverse dependence of fracture strain on degree of triaxiality.

The transverse stress perpendicular to the plane of the interface (σ_{xx} in the arrester orientation, σ_{zz} in the divider orientation) will produce strains in both the base alloy (ε_b) and the interface material (ε_i). The stress will be the same in both materials but the plastic strains ε_i in the softer interface material are much greater than in the base material (Fig. 35). Fracture of the interface will occur if the strain ε_i reaches the critical strain for fracture ε_f before $K_I = K_{Ic}$. This requires that the transverse stresses (σ_{xx} or σ_{zz}) reach the fracture stress of the interface σ_f before K_I reaches K_{Ic} for fast crack propagation.

The maximum transverse stresses ahead of a crack occur at the elastic/plastic interface and are given by:[10]

$$\sigma_{xx} = \sigma_Y \left[\ell n \ (1+R/\rho)\right] \qquad (6)$$

$$\sigma_{zz} = \nu\sigma_Y \left[1+2 \ \ell n \ (1+R/\rho)\right] \qquad (7)$$

where σ_Y is the yield strength of the material, ν is poisson ratio , R is the plastic zone size and ρ is the notch root radius. For sharp cracks $\rho = \rho_o$. From sharp crack fracture mechanics:[13]

$$R/\rho = \frac{R}{\rho_o} = \frac{1}{3\pi\rho_o} \left(\frac{K_I}{\sigma_Y}\right)^2 \tag{8}$$

and substituting in equations (6) and (7):

$$\sigma_{xx} = \sigma_Y \left[\ln \left(1+ \frac{1}{3\pi\rho_o} \left(\frac{K_I}{\sigma_Y}\right)^2\right)\right] \tag{9}$$

$$\sigma_{zz} = \nu\sigma_Y \left[1+2 \ln \left(1+ \frac{1}{3\pi\rho_o} \left(\frac{K_I}{\sigma_Y}\right)^2\right)\right] \tag{10}$$

Delamination will occur when

$$\sigma_{xx} = \sigma_f = \sigma_Y \left[\ln \left(1+ \frac{1}{3\pi\rho_o} \left(\frac{(K_I)_s}{\sigma_Y}\right)^2\right)\right] \quad \text{(arrester)} \tag{11}$$

$$\sigma_{zz} = \sigma_f = \nu\sigma_Y \left[1+2 \ln \left(1+ \frac{1}{3\pi\rho_o} \left(\frac{(K_I)_s}{\sigma_Y}\right)^2\right)\right] \quad \text{(divider)} \tag{12}$$

Where $(K_I)_s$ is the critical stress intensity factor required for splitting (delamination), i.e., that necessary to obtain the critical fracture strain ε_f in the interface material. Delamination will occur <u>before</u> fast crack propagation if

$$(K_I)_s \leqq K_{Ic} \tag{13}$$

From equations (11) and (12) it is possible to solve for the critical stress intensity factor required for delamination:

$$\begin{aligned} (K_I)_s &= \left[3\pi\rho_o \sigma_Y^2 \left[\exp[\sigma_f/\sigma_Y] - 1\right]\right]^{1/2} \quad \text{(arrester)} \\ (K_I)_s &= \left[3\pi\rho_o \sigma_Y^2 \left[\exp[(\sigma_f-\nu\sigma_Y)/2\nu\sigma_Y] - 1\right]^{1/2} \quad \text{(divider)} \end{aligned} \tag{14}$$

The yield strength for the composite material may be determined by the law of mixtures:

$$\sigma_Y = (\sigma_Y)_b \, (V_f)_b + (\sigma_Y)_i \, (1 - (V_f)_b) \qquad (15)$$

where $(\sigma_Y)_b$ and $(\sigma_Y)_i$ are the yield strength of the base alloy and interface material respectively and $(V_f)_b$ is the volume fraction of the base material. Where a thin interface is used there is little difference between $(\sigma_Y)_b$ and σ_Y and σ_Y can therefore be approximated by $(\sigma_Y)_b$.

Using suitable values for ν, ρ_o, and σ_Y, the critical stress intensity factor required for delamination, $(K_I)_s$ may be determined as a function of fracture strength of the interface. Figure 36 shows this curve for both the arrester and divider orientations, in both the solution treated (σ_Y = 160) and annealed (σ_Y = 130 ksi) conditions. We have taken a handbook value of ν = 0.35 and have assumed ρ_o = 0.003", which is typical for high yield strength materials. We observe that delamination is favored in the arrester orientation, for both heat treated and annealed material.

SECTION VIII

PARAMETERS WHICH AFFECT DELAMINATION

From the previous discussion, there are six basic physical and mechanical properties which can affect the delamination process.

1) Fracture Toughness of the Base Alloy, $(K_{Ic})_b$

An increase in K_{Ic} for the base alloy will allow for a higher K_I before fast fracture will initiate. The result is an increase in the transverse stress and a corresponding increase in the interfacial strain. Therefore, a high K_{Ic} will increase the possibility of delamination, if all other parameters in equations (13) and (14) are held constant.

2) Yield Strength of the Base Alloy, $(\sigma_Y)_b$

The yield strength of the composite may be approximated by the base metal yield strength if a thin interleaf is used, as in the present experiments. Equation (14) indicates that an increase in σ_Y tends to both increase (pre-exponential term) and decrease (exponential term) $(K_I)_s$. Since the exponential term dominates, $(K_I)_s$ decreases with increasing yield strength σ_Y.

In high strength materials, the fast fracture toughness K_{Ic} decreases with increasing σ_Y. Since only one base alloy was used in the present work, it was not possible to study independently the effect of yield strength or fracture toughness of the base alloy. Results obtained from Billet #3 with the .005 inch titanium foil show the combined effect of these two base alloy material properties. Whereas no delamination occurred in the annealed material ($\frac{K_{Ic}}{\sigma_y} = .55$), the heat treated specimens with a higher yield strength and slightly lower K_{Ic} did delaminate ($\frac{K_{Ic}}{\sigma_y} = 0.35$). These results would indicate that increases in σ_Y favor delamination if K_{Ic} is not lowered too greatly.

3) Sheet Thickness of the Base Alloy, (t_b)

The thickness of the base alloy has little effect on the delamination process of the composite material. An increase in thickness will increase the composite yield strength slightly (larger volume fraction of base material, equation 10). In most cases this effect will be minimal.

As discussed previously, fracture toughness K_c is a function of the thickness of the material. Fracture toughness increases to a maximum at a thickness t#, then decreases with further increase in thickness until the plane strain value K_{Ic} is reached (Fig. 2). The initial increase in thin sheets has been attributed by Hahn and Rosenfield[14] to an increase in the volume of metal being deformed per unit cross section area of crack surface. The decrease in toughness at thicknesses greater than t# is caused by an increase in the area which fractures in a flat manner (plane strain) relative to the area which fractures by shear lip (plane stress).

When delamination into thin sheets occurs in the divider orientation, the toughness of the divided laminate will be equal to the toughness of the thin sheet of given thickness, t. For maximum toughness in the divider orientation, the base alloy thickness should be chosen as the thickness t# where K_c is maximum.

Although delamination occurred in the divider orientation of several billets in the experimental program, there was little change in toughness over wrought plate. Figure 37 shows a curve for K_c as a function of thickness for 6Al-4V titanium. Although the data does not extend down to the .040 inch thickness used in the present work, K_c for this thickness is well below the maximum value of 160 ksi $\sqrt{in}$. When delamination occurs

in these materials, the fracture toughness measured will be the K_c for the thickness of base material used in the composite. For this work, the K_c value for a base metal thickness of .040 inches can be found from the fracture toughness data for billets where delamination took place. By using this value as another point on Figure 37 and drawing a representative curve it is evident that the .040 inch material is well below the optimum. Had thicker sheets of the base metal (approximately 0.15") been chosen for this program, increases in toughness should have theoretically been obtained in the divider orientation.

4) Specimen Thickness, (B)

In very thin specimens where no triaxiality is obtained (plane stress deformation), no delamination would be expected to take place. Once the specimen is of sufficient thickness such that plane strain conditions are present, there should be no effect of specimen size on the delamination process. Experimentally this has been shown with Billets #2 and #4. Delamination and splitting occurred in both the small Charpy specimens as well as the larger compact tension specimens tested by AFML. In both cases, sufficient transverse stresses were present prior to splitting and delamination occurred.

5) Thickness of the Interface Material, (t_i)

As the thickness of the interface material is decreased the triaxial constraint in the interface increases. This was shown by West et al.[12] for braze joints under uniaxial loading. When the triaxiality of the interface is increased the theory of McClintock[11] predicts that the critical strain for fracture, ε_f, will decrease. Thus a lower stress intensity factor will be necessary to initiate delamination. Therefore

a decrease in interface thickness will increase the possibility of delamination.

This effect has been shown experimentally. For the arrester orientation, the heat treated material containing .010 inch titanium foil did not delaminate while the thinner .005 inch foil did delaminate and arrest the crack. No attempt to optimize the interface thickness was made in the present program.

6) Fracture Strength of the Interface Material, (σ_f)

A change in yield strength of the interface will change the stress-strain relation shown in Figure 35. A decrease in yield strength will generally lower the fracture stress σ_f for a given ductility ε_f. This will reduce the stress intensity factor required for delamination (Fig. 36). The effect of variations in interface yield strength or fracture strength was not studied independently. The combined effect of interface thickness and yield strength can be determined by comparison of the results for Billet #3 and #6. Where no delamination occurred with the higher yield strength, thicker titanium interleaf, delamination and splitting did take place with the thin, low yield strength aluminum foil interleaf.

A second factor which governs the fracture strength is the ductility of the interface. For the same yield strength, an interface with lower ductility will have a lower fracture strength since less strain will be necessary for fracture. Therefore as the ductility of the interface is decreased, the greater the chance for delamination. This has been shown experimentally where the microvoid interfaces were used. Delamination and splitting occurred in almost all cases due to the restricted deformation zone of this type of interface. A low ductility adhesive material used

as an interface, although not tested experimentally, would also show this behavior.

The effect each of these six physical and mechanical properties has on the delamination characteristics of the multi-laminate composite is summarized in Table XII.

SECTION IX

CONCLUSIONS AND RECOMMENDATIONS

The use of composite materials consisting of lamella of 6Al-4V titanium with a weak interface has been shown to be an effective way of increasing the toughness of high strength Ti 6Al-4V material. Two types of interface were utilized, microvoid sheets and a thin foil. From the reliability standpoint, the foil type of interface with a full strength diffusion bond is superior to the controlled porosity diffusion bond which is weakened by the presence of microvoids. During billet fabrication, the formation of a uniform distribution of microvoids is difficult to achieve and therefore the strength of the interface varies from one area to another. Comparison of the NAR tensile data for Billet #2 with that made by AFML makes this point apparent. This discrepancy in results may be explained by the fact that the tensile specimens came from two different areas of the fabricated billet. The use of a full strength bond where there is no microvoid formation is much more desirable because there are fewer problems with quality control of the bond itself.

The use of controlled diffusion bonding as an effective means of increasing toughness has been attempted in this study and in past experimentation. In the arrester geometry the toughness is much higher if delamination occurs and gross yielding follows. In the divider orientation splitting could increase the fracture toughness to K_c for the sheet thickness used in the composite. This increase in turn leads to an increase in the critical crack size for the material. For example, assume the maximum K_c for 6Al-4V titanium is 160 ksi $\sqrt{in.}$ (Fig. 37). From Table IX the K_Q for full strength material is approximately 80 ksi $\sqrt{in.}$ Therefore

K_c is approximately doubled and from equation (4) the critical crack size will be increased four times when delamination and splitting occur.

A second effect which can occur in laminate composites has a greater consequence. Assume we have a flaw which becomes the initiation site of a crack, which then grows at a certain cyclic stress level. This flaw may be a surface flaw as shown by points A and B in Figure 38 or an internal flaw as shown by point C. As these cracks grow toward the interface, delamination at the interface will occur if the stress intensity factor, K_I, is of sufficient magnitude $(K_I)_s$. If delamination takes place then the crack is effectively channeled. As long as the area of the crack is a small fraction of the cross section of the load bearing member, overloading of the remaining area will not take place. The structure is essentially composed of a series of redundant elements. This is of significant value in aerospace structures where redundancy in design is required to meet fail-safe criteria. By use of laminate composite materials the redundancy is built into the material itself, rather than through the use of dual, full size structural elements (e.g., wing attachment lugs).

Another significant advantage of a laminate composite containing a weak interface is the superior load carrying capacity in the transverse direction. From results of this study, using an aluminum interleaf foil where delamination occurred, this transverse to longitudinal ratio is .26. With further optimization of the interface material (i.e., thinner titanium foil), a high ratio should be obtainable.

The use of a multi-laminate composite containing weak interfaces has a great potential for practical applications. Optimization of the composite may be possible through consideration of the factors discussed in Section VIII. From these parameters, thin interleaf materials with relatively low yield strengths seem desirable. Also for maximum increase of toughness in the divider orientation, the base metal thickness should be chosen so that K_c is maximum. Further work is necessary to determine what materials and thicknesses should be used to obtain the maximum increase in toughness while maintaining a good ratio of transverse to longitudinal strength. While the six parameters discussed will help in the optimization process, other factors must be considered. These include cost, ease of bonding, and other fabrication problems. Further work on the fatigue properties and the stress corrosion characteristics is also necessary before these types of materials may be applied to practical applications.

REFERENCES

1. Almond, E.A., J.D. Embury, E.S. Wright, Interfaces in Composites, ASTM STP 452, 1969, pp. 107-129.

2. Kaufman, J.G., Quarterly Transactions ASME, Journal of Basic Engineering, Vol. 89, Series D, 1967, pp. 503-507.

3. Birkbeck, G., N.J. Petch, A.E. Wraith, "The Fracture of Laminated Pressurized Containers," unknown.

4. Leighter, H.L., Journal of Spacecraft and Rockets, Vol. 3, 1966, pp. 1113-1120.

5. Embury, J.D., N.J. Petch, A.E. Wraith, E.S. Wright, Transactions of The Metallurgical Society of the AIME, Vol. 239, 1967, pp. 114-118.

6. McCartney, R.F., R.C. Richard, P.S. Trozzo, Transactions of the ASM, Vol. 60, 1967, pp. 384-394.

7. Brown, W.F., and J.E. Srawley, Plain Strain Crack Toughness Testing of High Strength Metallic Materials, ASTM STP 410, 1966, p. 13.

8. Saxton, H.J., A.J. West, C.R. Barrett, Metallurgical Transactions, Vol. 2, 1971, pp. 999-1007.

9. Harrigan, M.J., A.W. Sommers, G.A. Alers, "The Effect of Texture on the Mechanical Properties of Titanium Alloys," North American Rockwell Report No. 69-909, 1969.

10. Tetelman, A.S. and A.J. McEvily, Fracture of Structural Materials, John Wiley & Sons, Inc. 1967.

11. McClintock, F.C., Journal of Applied Mechanics, Vol. 35, 1968, p. 363.

12. West, A.J., H.J. Saxton, A.S. Tetelman, C.R. Barrett, Metallurgical Transactions, Vol. 2, 1971, pp. 1009-1017.

13. Malkin, J., and A.S. Tetelman, Engineering Fracture Mechanics, Vol. 3 No. 2, 1971, pp. 151-169.

14. Hahn, G.T., and A.R. Rosenfield, Applications Related Phenomena in Titanium Alloys, ASTM STP 432, p. 5.

15. Wilhelm, D.P., "Fracture Mechanics Guidelines for Aircraft Structural Applications," Technical Report AFFDL-TR-69-111, 1970.

16. Hahn, G.T., and A.R. Rosenfield, "Plastic Flow in the Locale on Notches and Cracks in Fe-3Si Steel Under Conditions Approaching Plane Strain," Final Report of Project SR-164, Bureau of Ships Contract NObs-92383.

APPENDICES

APPENDIX I

TABLES

TABLE I

Physical Properties of .040 inch Ti-6Al-4V Material Used in the Study

HEAT	YIELD STRENGTH (ksi)	TENSILE STRENGTH (ksi)	ELONGATION in 2"(%)
1	139.5	146.5	13.0
2	138.1	146.1	11.6
3	135.0	142.0	14.5
4	133.2	142.9	13.0

TABLE II

Chemical Analysis of .040 inch Ti-6Al-4V Material Used in the Study

HEAT	C	Fe	Al	V	N_2	O_2	H_2
1	.023	.09	6.0	4.1	.013	.12	.005
2	.023	.10	6.0	4.1	.010	.13	.007
3	.023	.06	5.8	4.0	.008	.11	.004
4	.023	.07	5.9	4.0	.009	.10	.005

TABLE III

Physical Properties of Titanium Foil Used as Interleaf Material

FOIL THICKNESS (inches)	YIELD STRENGTH (ksi)	TENSILE STRENGTH (ksi)	ELONGATION (%)
.005	84.7	94.2	24.7
.010	79	102	22.5

TABLE IV

Chemical Analysis of Titanium Foil Used as Interleaf Material

FOIL THICKNESS (inches)	C	Fe	N_2	O_2	H_2
.005	.06	.12	.047	.276	.0048
.010	.01	.30	.01	<.25	69 ppm

TABLE V

Basic Properties and Diffusion Bonding Parameters of the Billets

BILLET#	INTERLEAF MATERIAL	AS FABRICATED TENSILE STRENGTH OF BOND** Avg. of two specimens	TIME (hrs.)	TEMPERATURE (°F)	PRESSURE (psi)
1	NONE (Full strength)	No tests made	5	1700	2000
2	NONE (Microvoid)	68 ksi	.75	1350	5000
3	.005" CP Ti foil	132 ksi	5	1700	2000
4*	NONE (Microvoid)	75 ksi	1.5	1400	5000
5	.010" CP Ti foil	125 ksi	5	1700	2000
6	.0015" Al foil	38 ksi	3	1000	6000

* Billet #4 specimens were given a thermal treatment of 1/2 hour at 1600°F with no applied pressure which raised the bond strength to 142 ksi.

** For complete tensile results, see Table 7.

TABLE VI

Mechanical Properties of Billet #4 Material After Heat Treatment at 1650°F (original bond strength 75 ksi)

SPECIMEN IDENTIFICATION	HEAT TREATMENT TIME at 1650°F(hr)	YIELD STRESS (ksi)	TENSILE STRESS (ksi)	% ELONGATION (1 inch)	% REDUCTION OF AREA
1	1/2	134.9	139.0	1	4
2	1	135.3	143.0	3	4
3	2	132.7	142.8	5	11
4	4	127.9	141.7	10	17
5	6	--	120.3	1/2	3
6	7-1/2	131.4	141.6	6	13

TABLE VII

North American Rockwell Tensile Specimen Test Results

(Bond Plane Perpendicular to Load Direction, As-Fabricated Material)

BILLET #	SPECIMEN #	YIELD STRENGTH (ksi)	TENSILE STRENGTH (ksi)	ELONGATION IN 1 INCH (%)	REDUCTION IN AREA (%)
1	----------	----------	No tests made	----------	----------
2	1	-	63.7	0	0
	2	-	73.0	0	0
3	1	124.9	132.9	9	17
	2	125.3	132.3	14	31
4	1	137	142.2	2	1.5
	2	135.6	142.3	2	1.6
5	1	112.1	124.3	11	28.1
	2	112.0	126.3	14	24
6	1	-	33.8	1/2	0
	2	-	43.4	1	0

TABLE VIII - AFML TENSILE TEST RESULTS

Billet No.	Orientation of Bond to Loading Direction	σ_y Ksi	Tensile Strength Ksi	Elongation %	R.A. %
1	Perpendicular	130.2	134.7	15.7	51.3
	Parallel	126.8	135.6	17.7	49.3
2	Perpendicular	-	46.0	.4	.5
	Parallel	143.3	146.8	13.9	50.8
3	Perpendicular	125.4	130.6	8.8	17.9
	Parallel	120.8	129.7	13.6	29.2
4	Perpendicular	136.5	138.4	.7	2.0
	Parallel	132.7	141.2	15.0	50.3

TABLE IX - FRACTURE TOUGHNESS RESULTS FROM PRECRACKED CHARPY SPECIMENS

Billet Number	Orientation	Fracture Toughness Ksi $\sqrt{in.}$	
		Annealed Condition	Heat Treated Condition
1	Arrester	76.4	51.1
	Divider	82.5	55.8
	Enhancer	75.7	37.9
2	Arrester	arrest	arrest
	Divider	73.4	60.7
	Enhancer	52.7	44.3
3	Arrester	82.5	arrest
	Divider	84.2	54.5
	Enhancer	59.0	32.7
4	Arrester	74.2*	arrest
	Divider	82.6	63.7
	Enhancer	73.5	33.9
5	Arrester	82.2	74.3
	Divider	83.6	59.4
	Enhancer	60.0	45
6	Arrester	arrest	--
	Divider	68.8	--
	Enhancer	48	--

*One Delaminated

TABLE X - AFML FRACTURE TOUGHNESS TEST RESULTS FROM COMPACT TENSION SPECIMENS

Billet No.	Specimen Orientation	K_Q Ksi $\sqrt{in}$
1	Arrester	63.9
	Divider	82.6
	Enhancer	60.4
2	Arrester	Shear along interface
	Divider	49.7
	Enhancer	Broke while fatiguing
3	Arrester	63.4
	Divider	80.4
	Enhancer	56.2
4	Arrester	Shear along interface
	Divider	68.7
	Enhancer	Broke during machining

TABLE XI - AFML FATIGUE TEST RESULTS

Billet No.	Orientation of Bond Plane to Load Direction	Stress Ksi	Cycles
1	Perpendicular	65	1.6×10^5
	Perpendicular	<65	0
	Parallel	65	4.9×10^6
2	Perpendicular	65	5.1×10^3
	Perpendicular	65	6.6×10^3
	Parallel	Broke during Machining	
3	Perpendicular	65	6.4×10^4
	Perpendicular	65	1.5×10^6
	Parallel	65	7.4×10^6
4	Perpendicular	65	5.2×10^4
	Perpendicular	65	5.5×10^5
	Parallel	65	1.0×10^7

TABLE XII - EFFECT OF VARIOUS PARAMETERS ON DELAMINATION CHARACTERISTICS OF LAMINATE COMPOSITES

Parameter		Significant Effect
Base Alloy Fracture Toughness	$(K_{Ic})_b$	Increase favors delamination
Base Alloy Yield Strength	$(\sigma_Y)_b$	Increase favors delamination
Base Alloy Sheet Thickness	$(t)_b$	Optimum gives maximum K_c
Specimen Thickness	B	None if plane strain conditions prevail
Interface Material Thickness	$(t)_i$	Decrease favors delamination
Interface Material Fracture Strength	σ_f	Decrease favors delamination

APPENDIX II

FIGURES

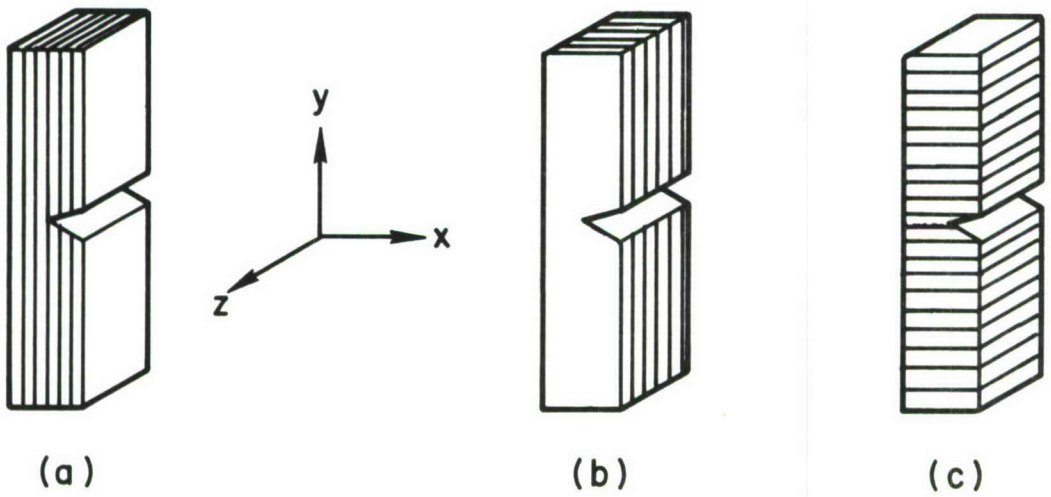

Figure 1. Possible Orientation of the Interface in Relation to the Propagating Crack: (a) Crack Arrester, (b) Crack Divider, (c) Crack Enhancer

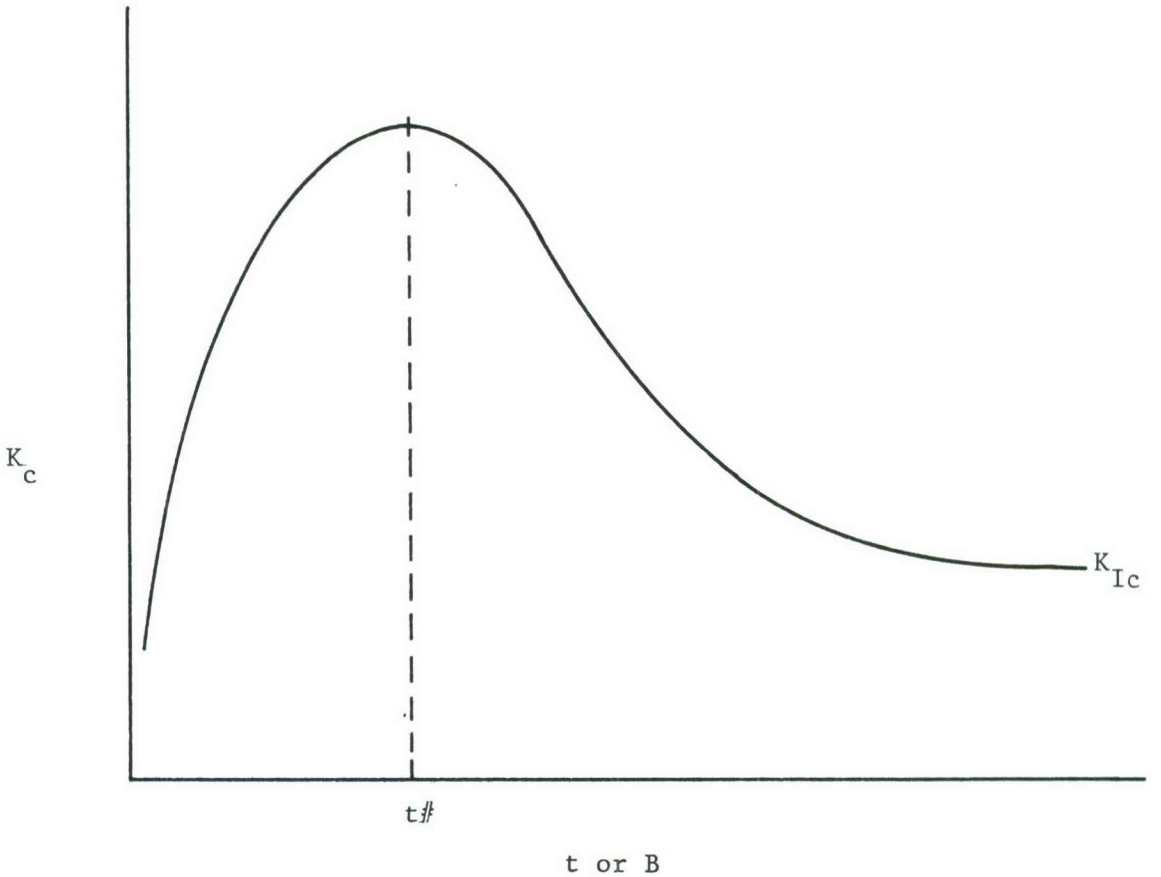

Figure 2 Variation of Fracture toughness with material thickness for most materials

Figure 3 Typical microstructure of Billet #1 (100X).

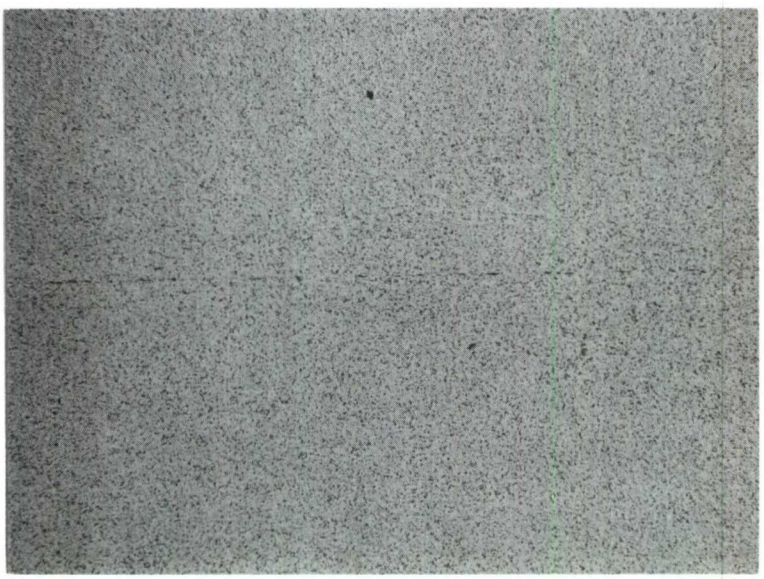

Figure 4a Typical microstructure of Billet #2 (100X).

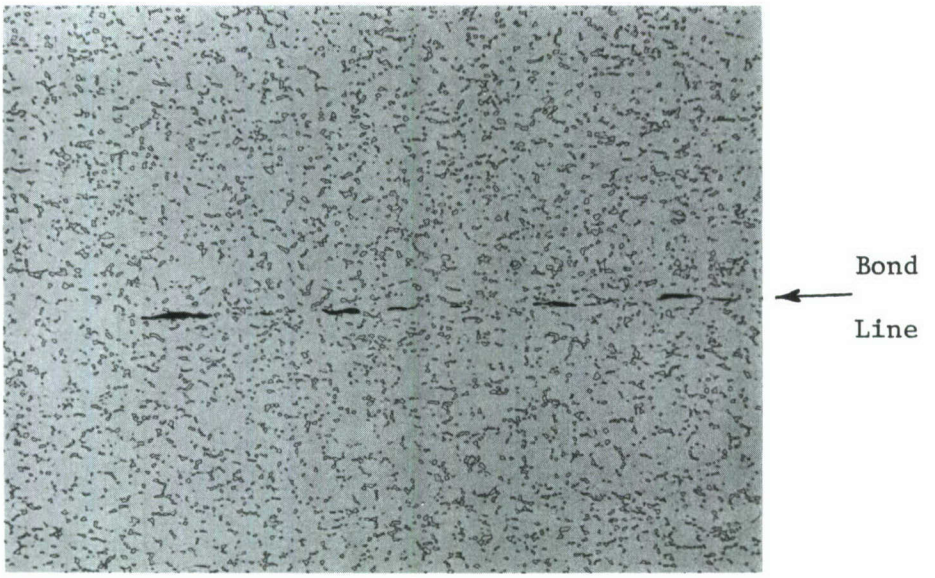

Figure 4b Typical microstructure of Billet #2 (500X).

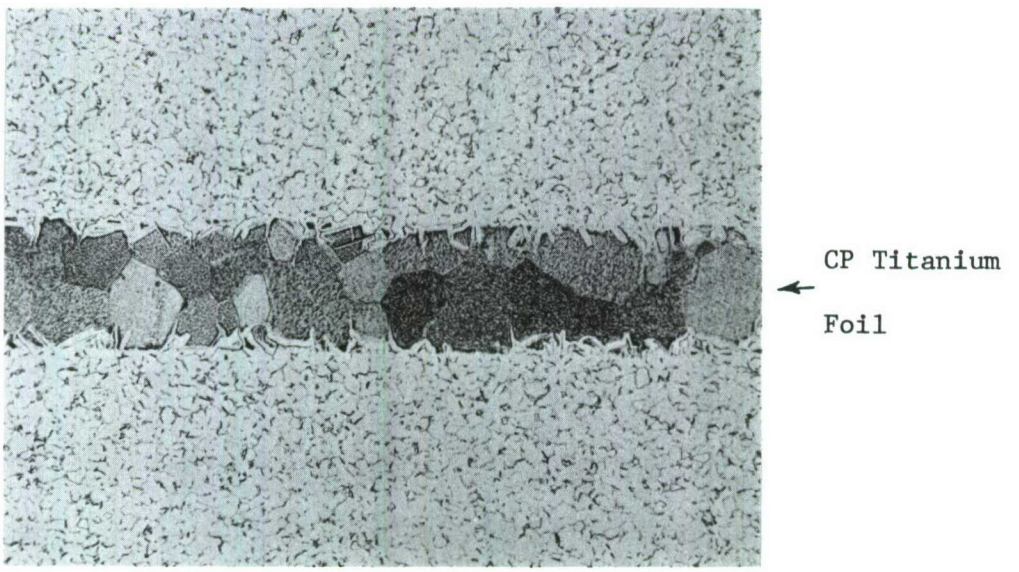

Figure 5 Typical microstructure of Billet #3 (100X).

(a)

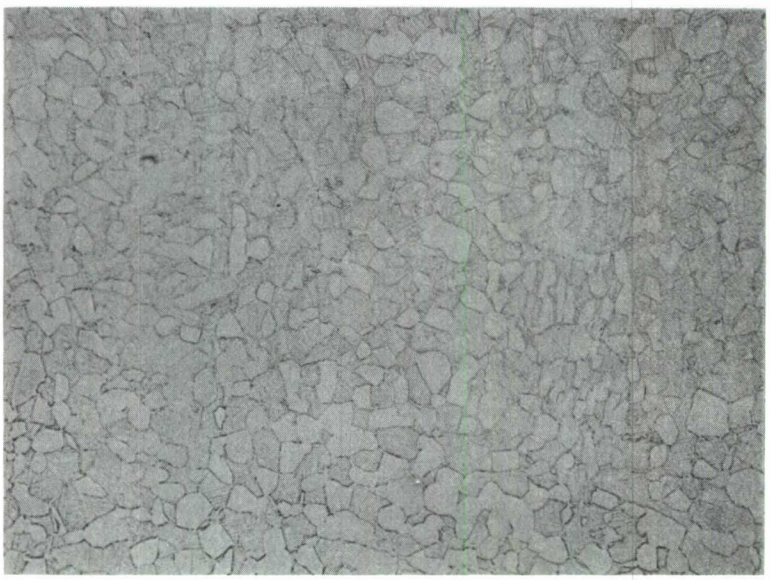

(b)

Figure 6 Typical microstructure of Billet #4 as fabricated (a) and after thermal treatment (b), (500X).

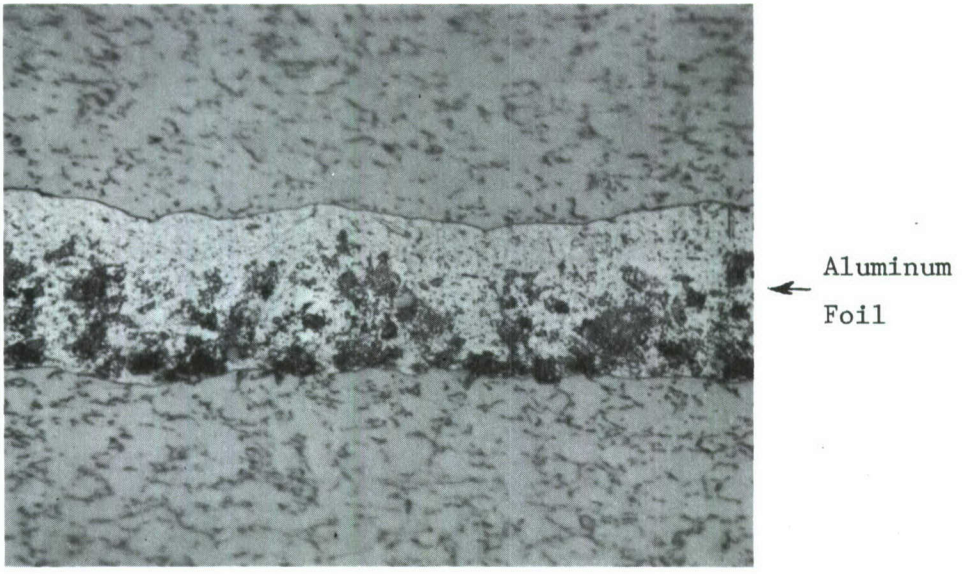

Figure 7 Typical microstructure of Billet #6 (500X).

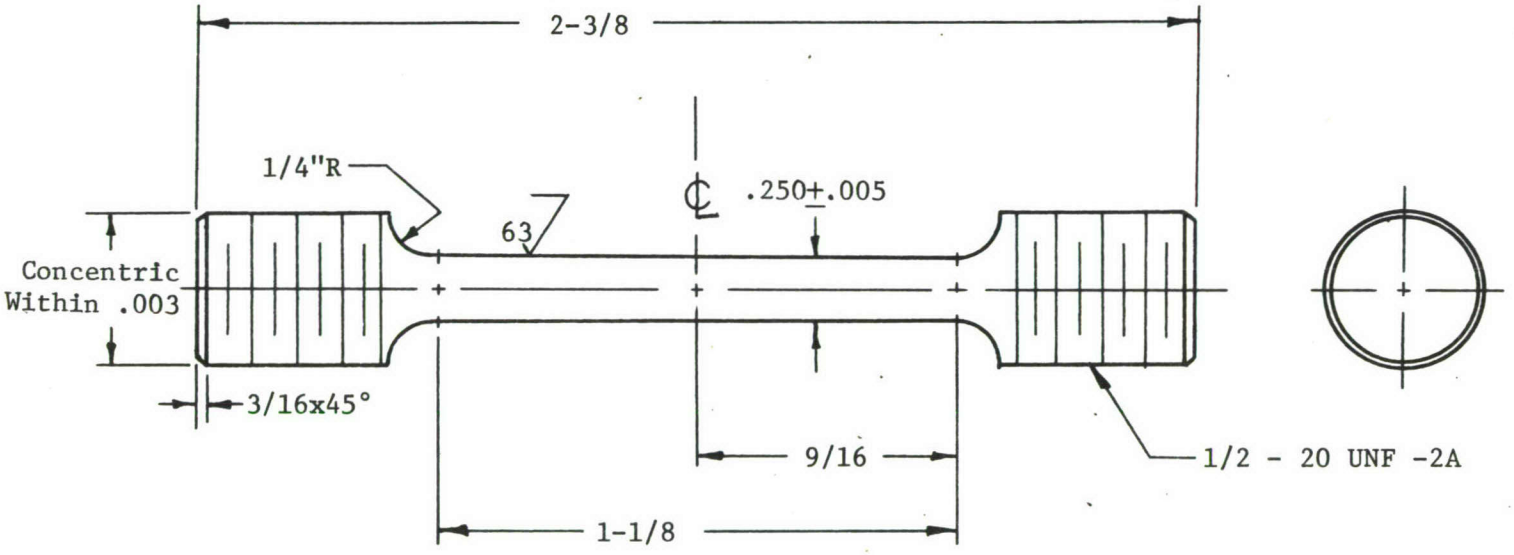

Figure 8 Tensile specimen used for NAR tensile tests.

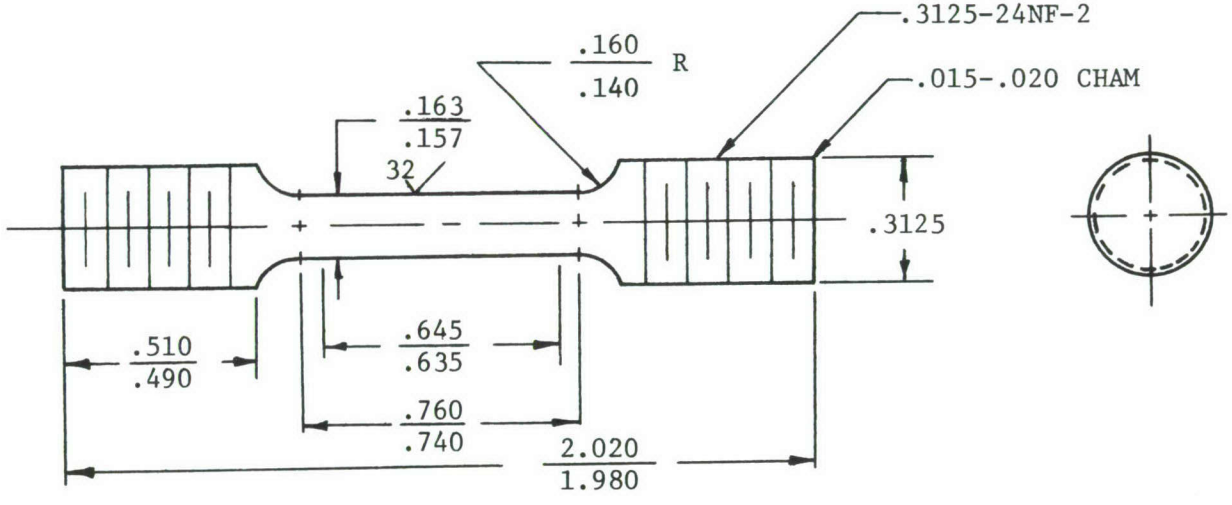

Figure 9 Tensile specimen used for AFML Tensile tests.

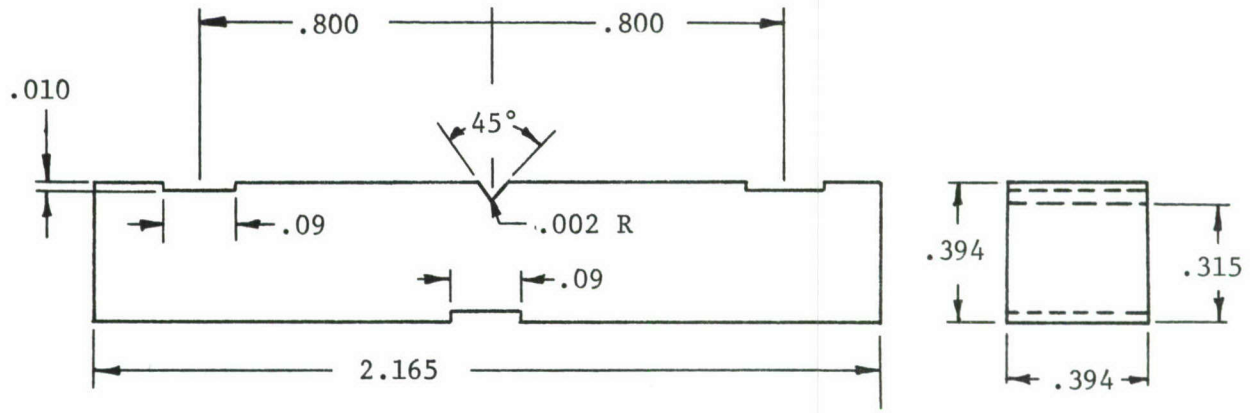

Figure 10 Charpy specimen used for fracture toughness testing.

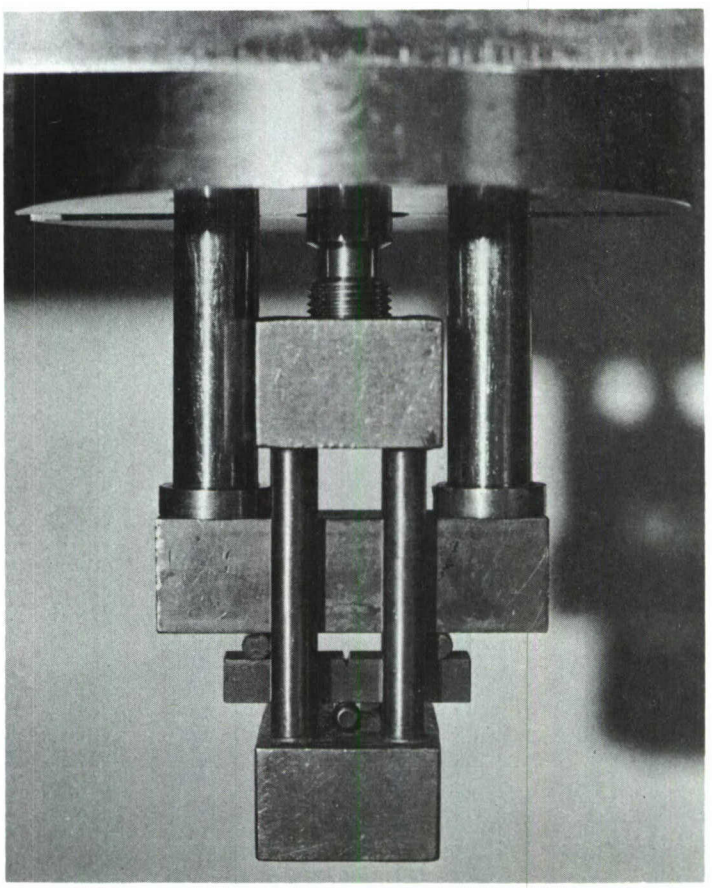

Figure 11 Photo of three point bend jig used for fracture toughness testing.

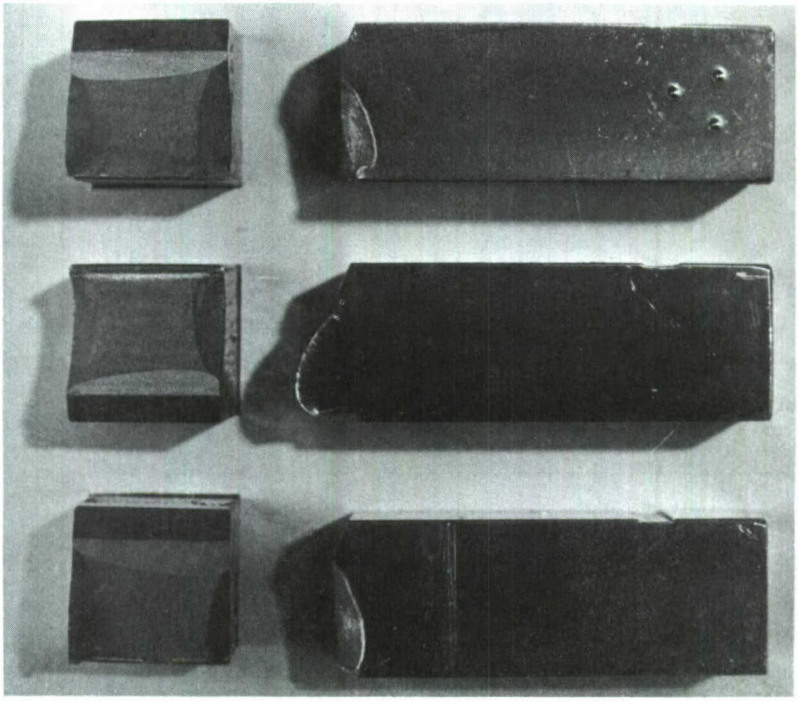

Figure 12 Typical fracture surface appearance of Billet #1 specimens.

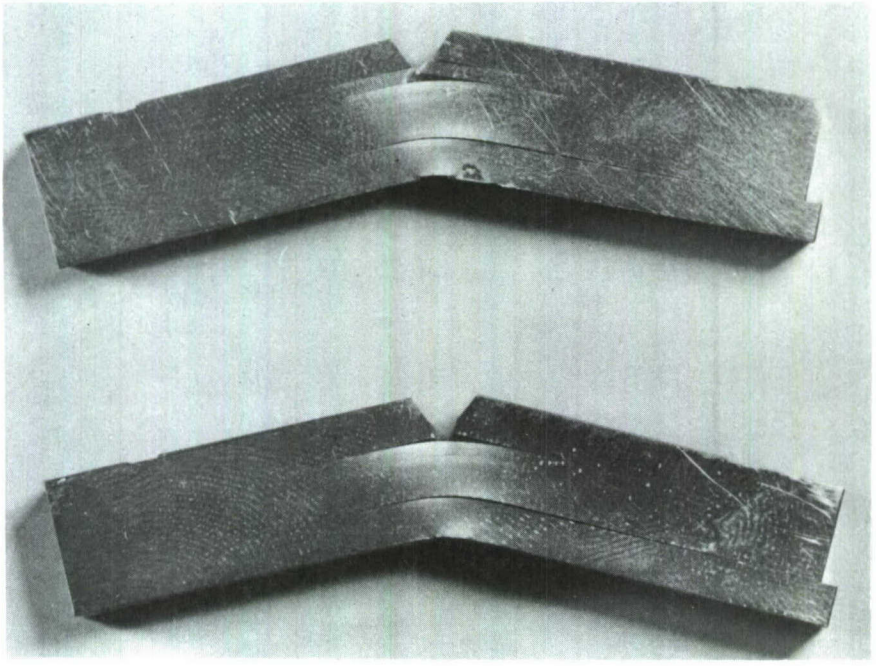

Figure 13 Delamination in arrester specimens of Billet #2.

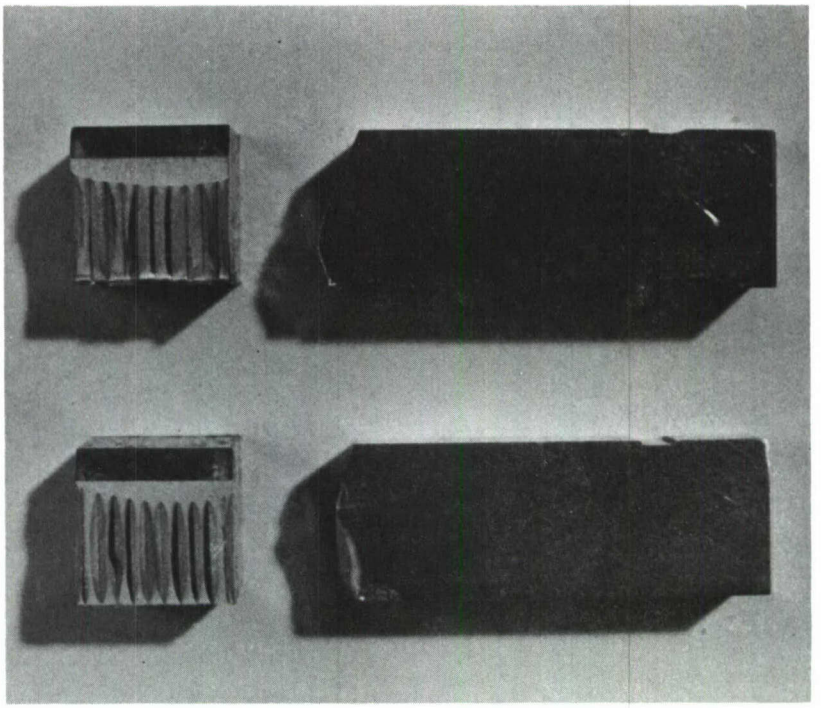

Figure 14 Delamination and splitting in divider orientation of Billet #2.

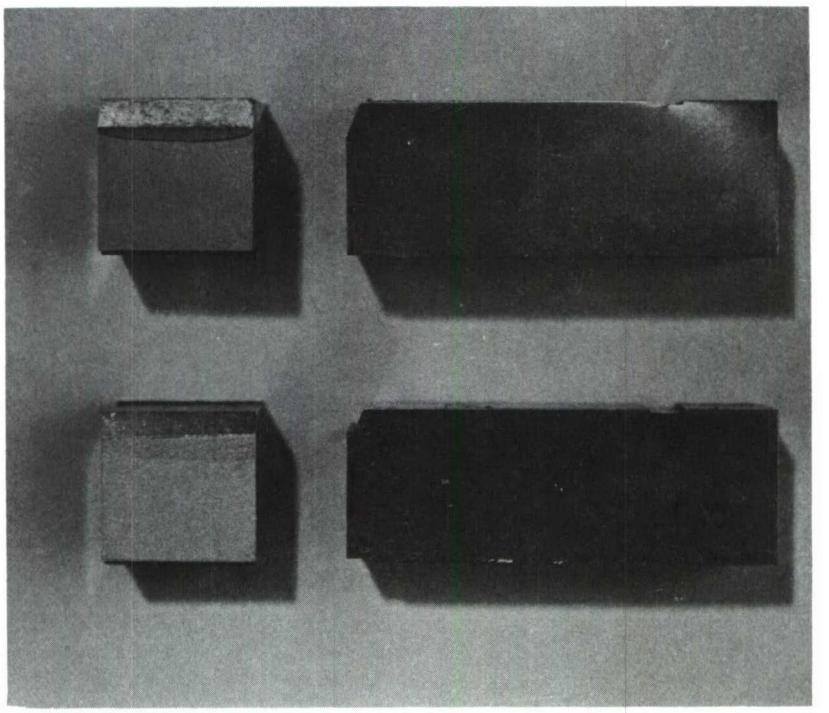

Figure 15 Fracture appearance for enhancer geometry of Billet #2.

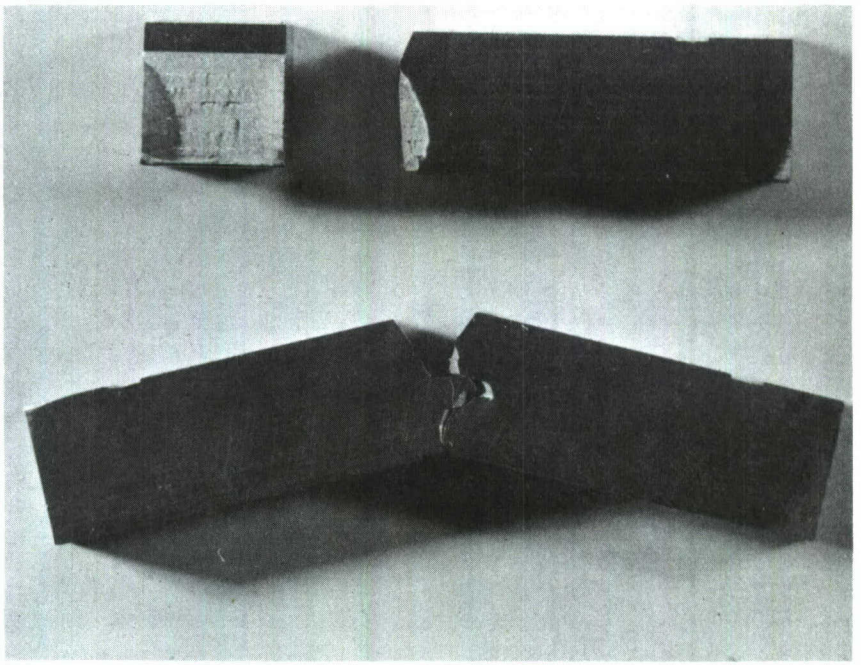

Figure 16 Fracture appearance in arrester orientation of Billet #3.

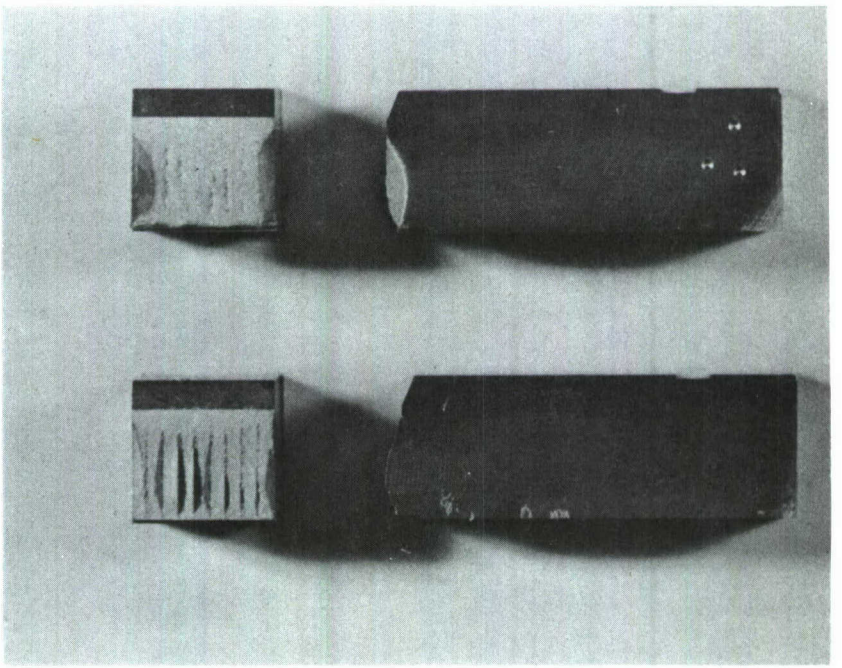

Figure 17 Fracture appearance in divider orientation of Billet #3.

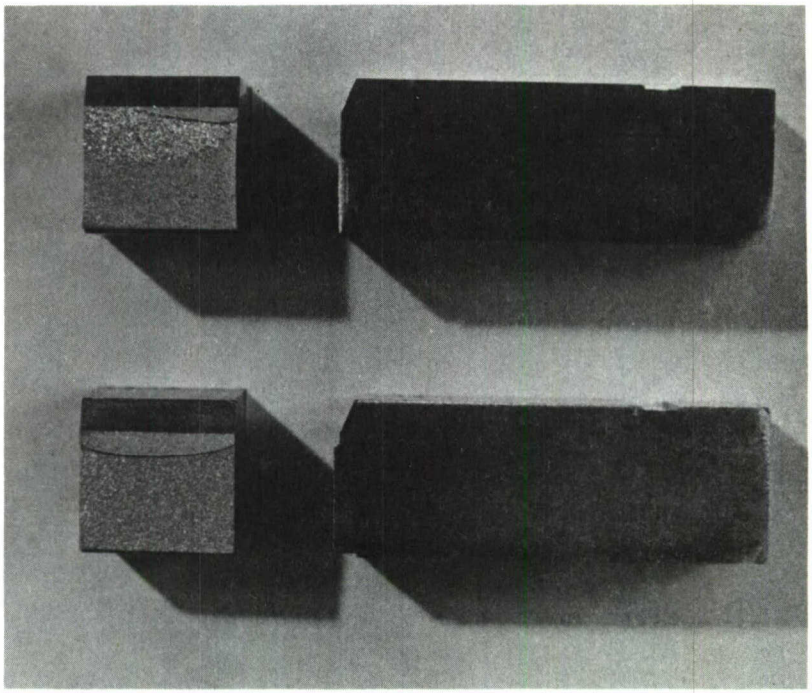

Figure 18 Fracture appearance in enhancer orientation of Billet #3.

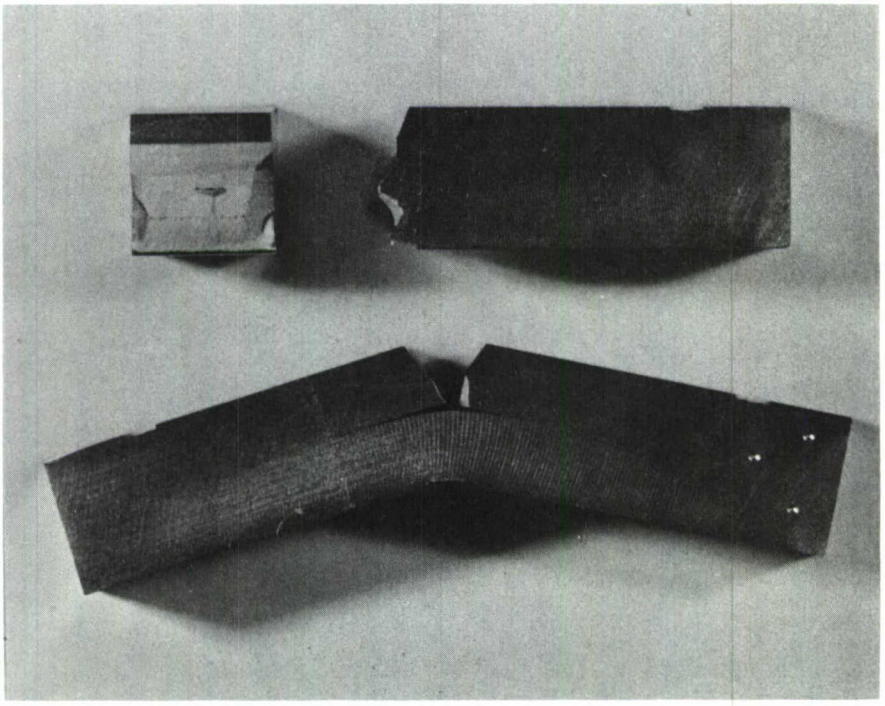

Figure 19 Fracture appearance in arrester orientation of Billet #4.

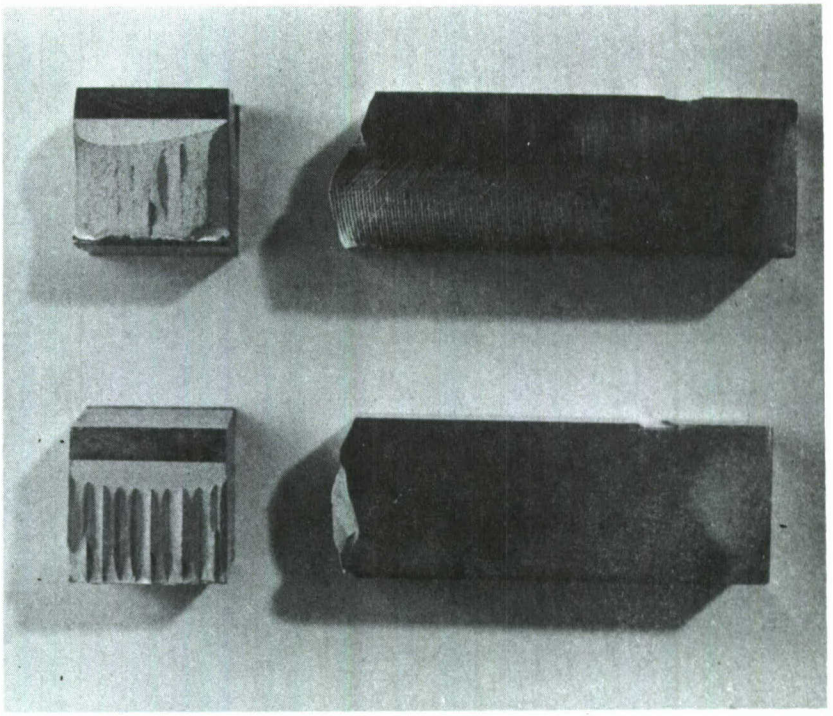

Figure 20 Fracture appearance in divider orientation of Biller #4.

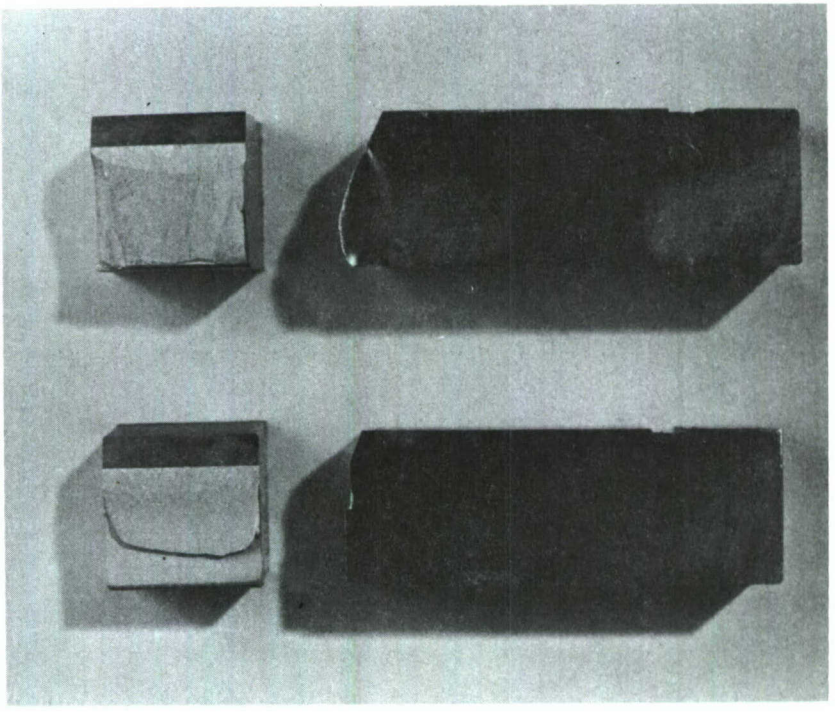

Figure 21 Fracture appearance in enhancer orientation of Billet #4.

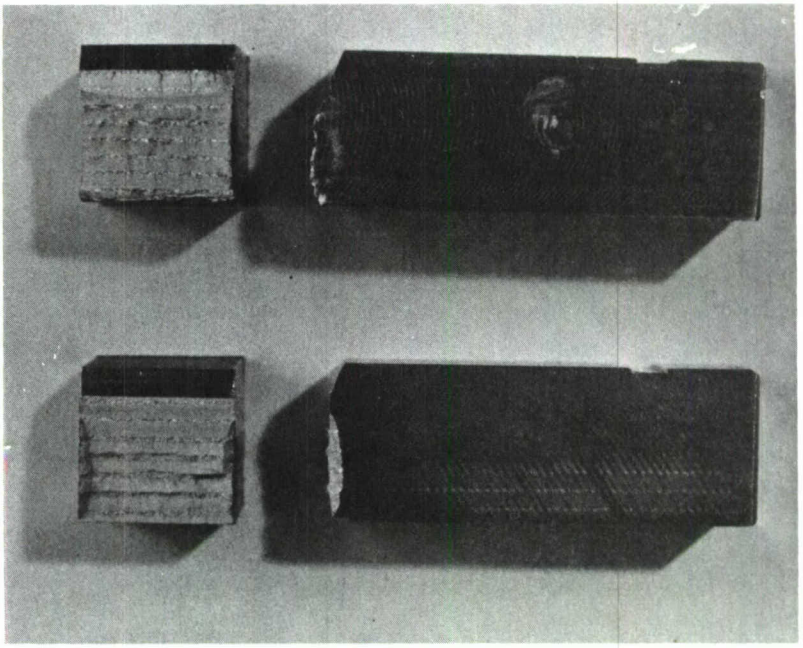

Figure 22 Fracture appearance in arrester orientation of Billet #5.

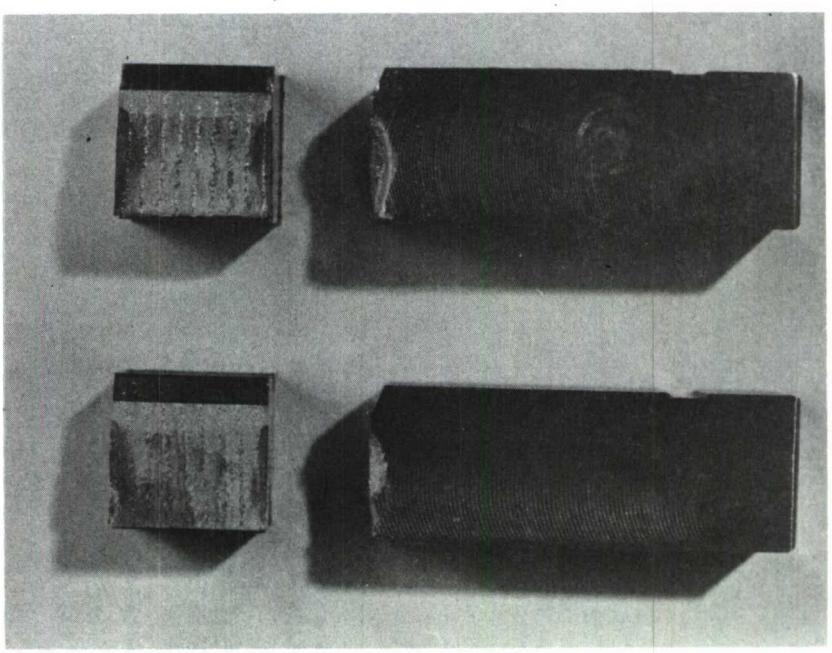

Figure 23 Fracture appearance in divider orientation of Billet #5.

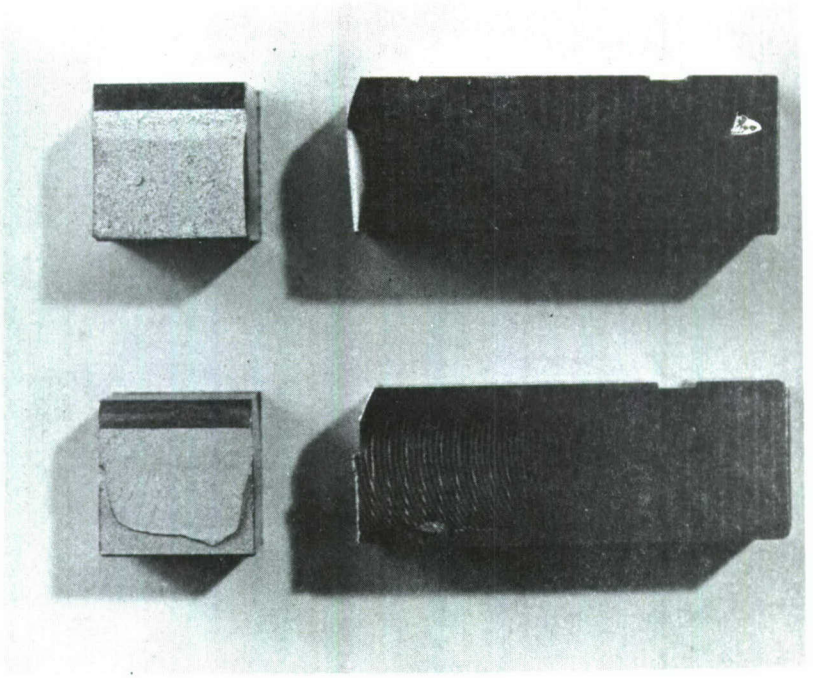

Figure 24 Fracture appearance in enhancer orientation of Billet #5.

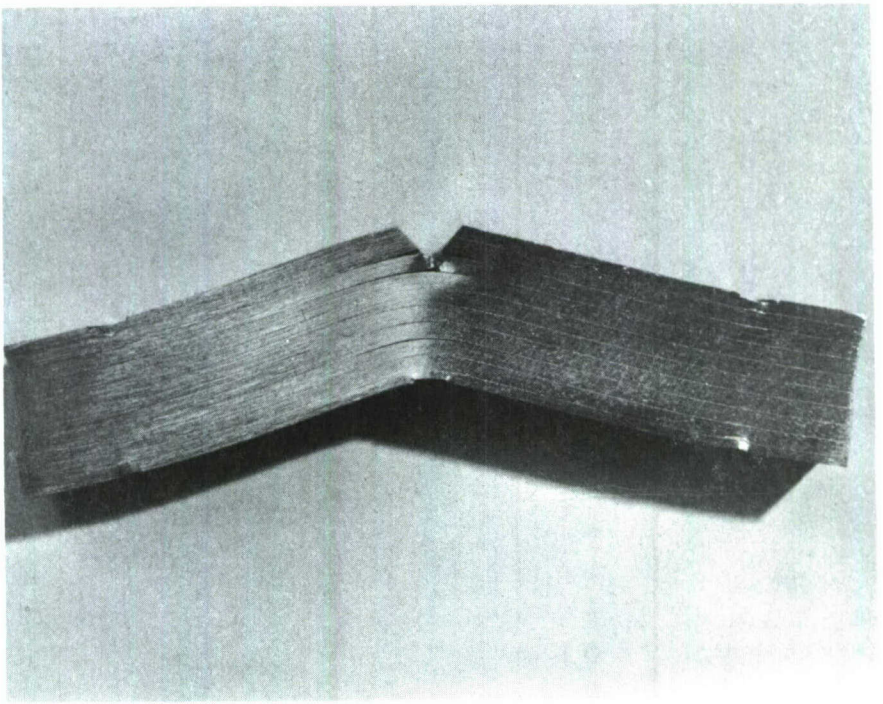

Figure 25 Delamination and crack arrest in arrester orientation of Billet #6.

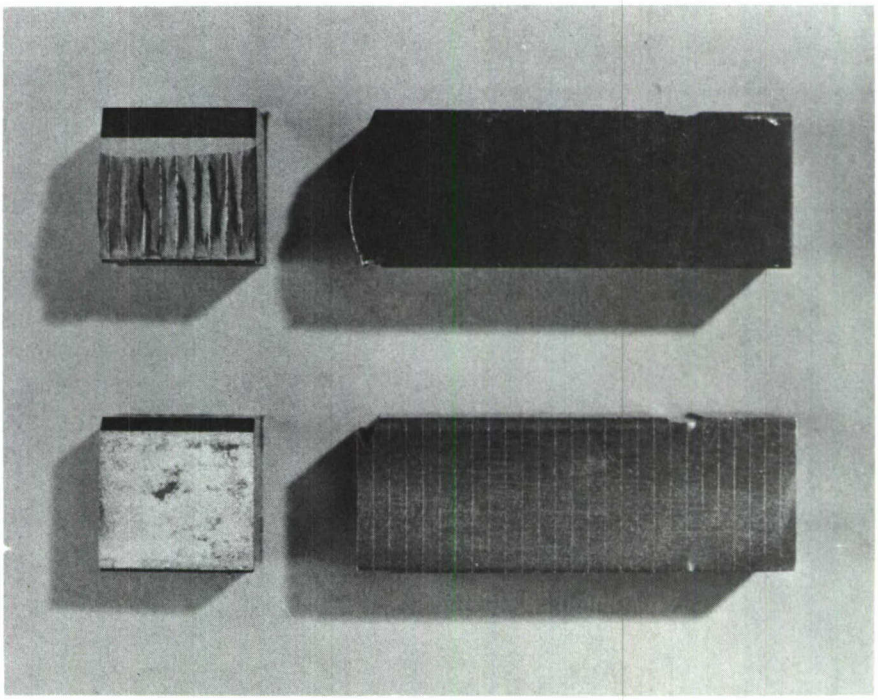

Figure 26 Fracture appearance of divider (top) and enhancer orientations of Billet #6.

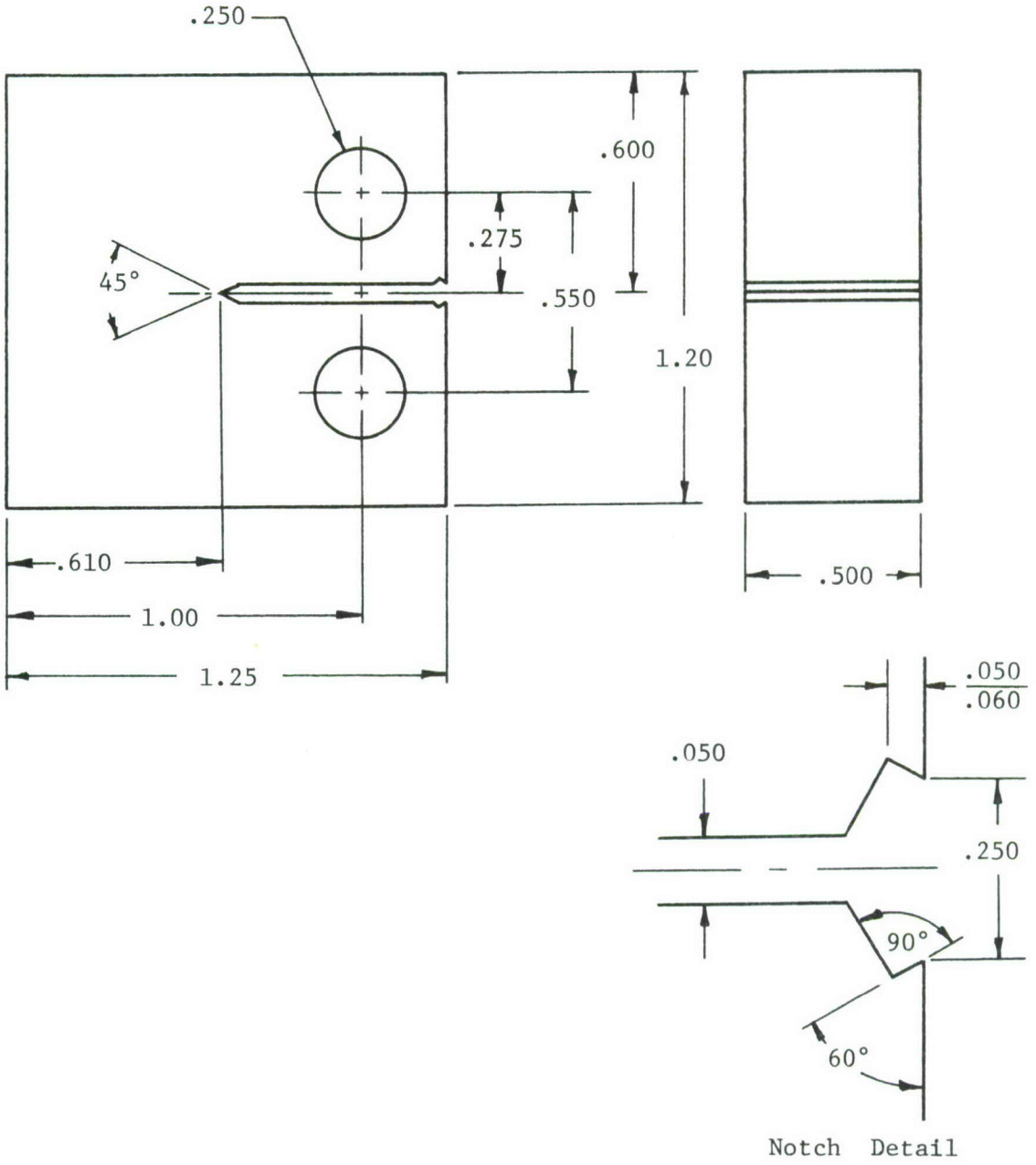

Figure 27 Half size compact tension specimen used for AFML fracture toughness testing.

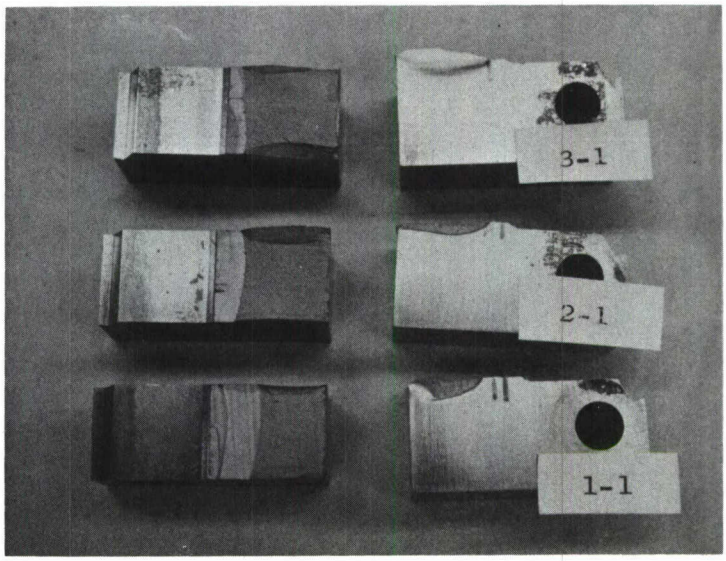

(a)

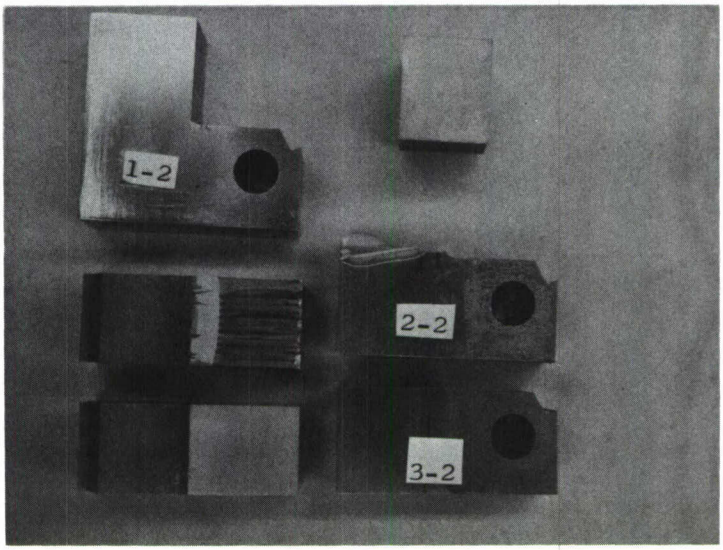

(b)

Figure 28 Fracture appearance of AFML toughness specimens for (a) Billet #1, (b) Billet #2, (c) Billet #3 and (d) Billet #4.

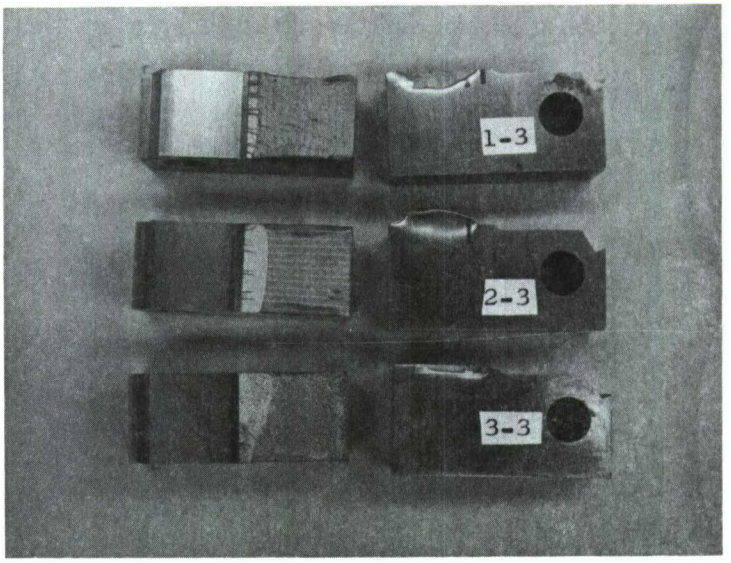

Arrester

Divider

Enhancer

(c)

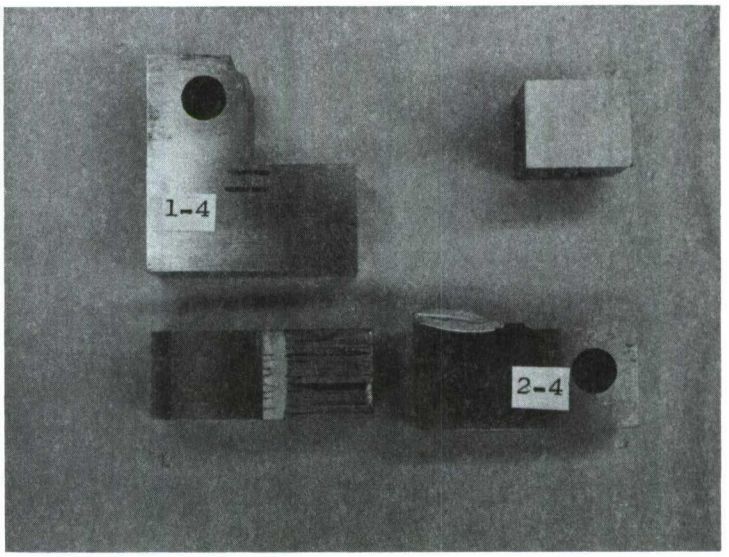

Arrester

Divider

(d)

Figure 28 Continued

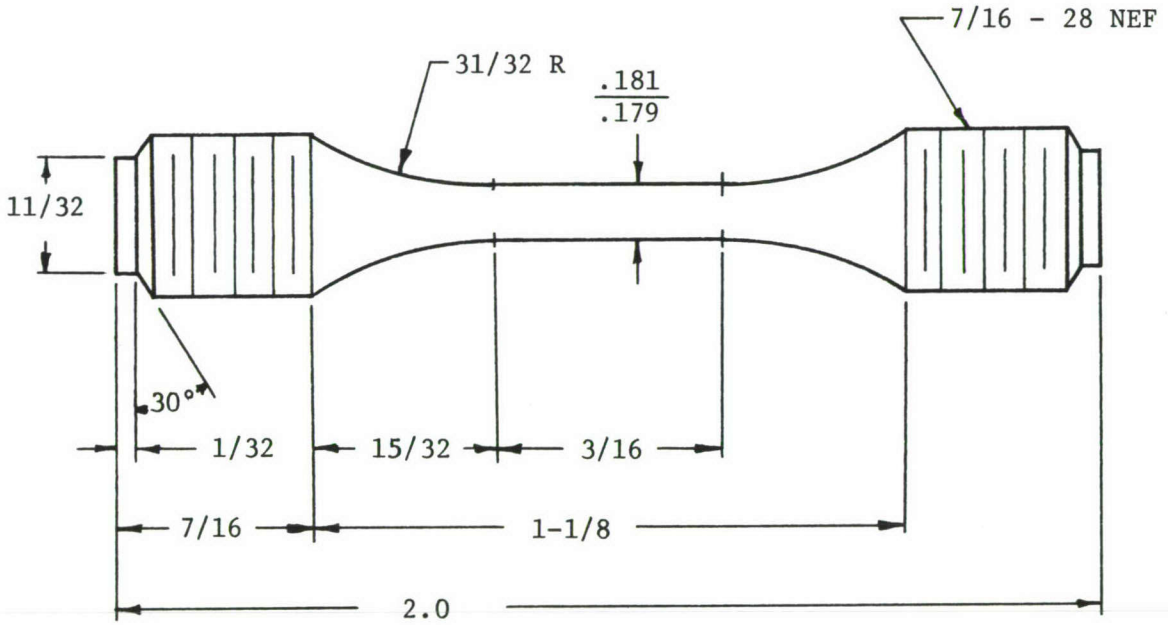

Figure 29 Fatigue specimen used in AFML fatigue testing.

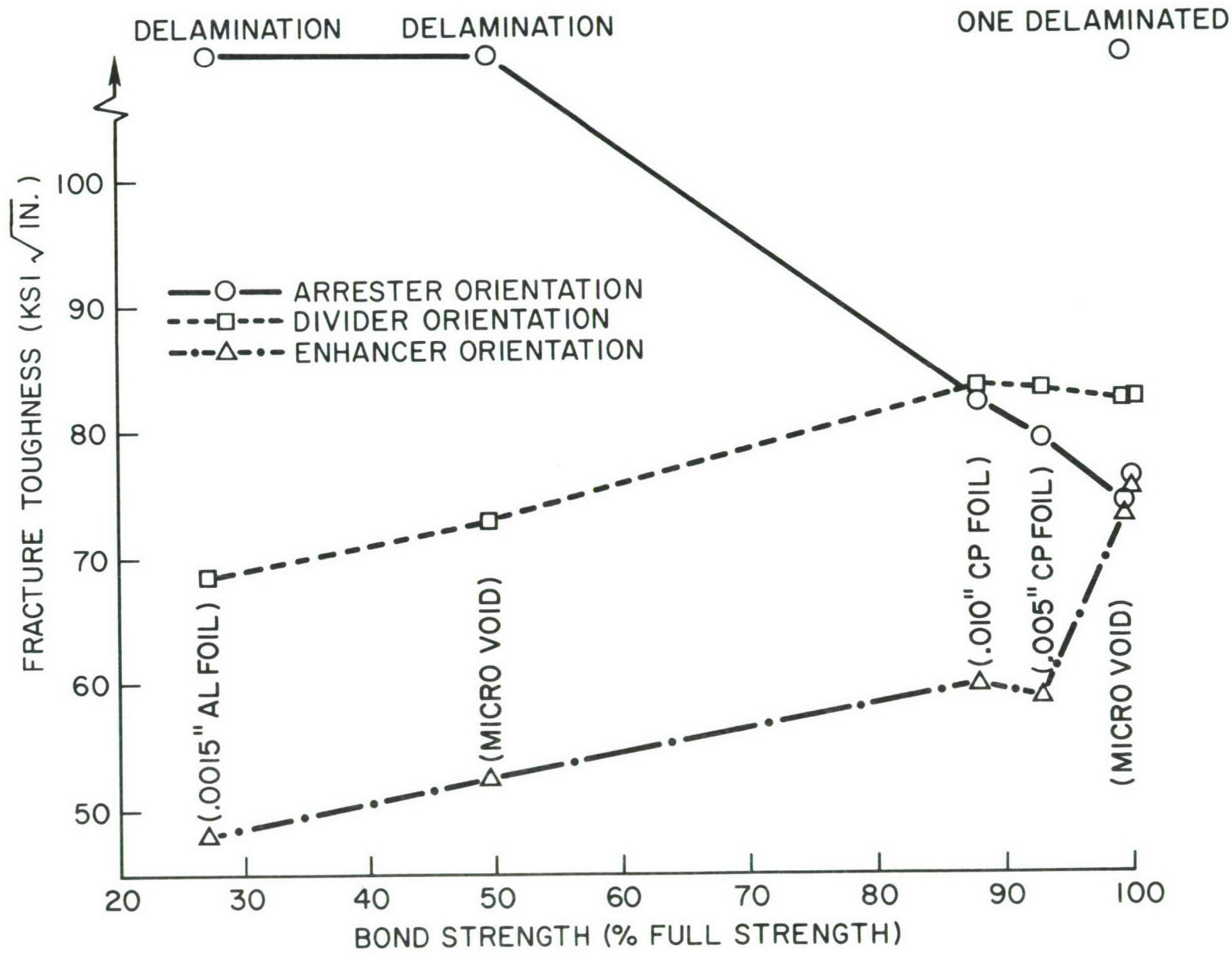

Figure 30. Fracture Toughness vs Relative Bond Strength for Material in the Annealed Condition

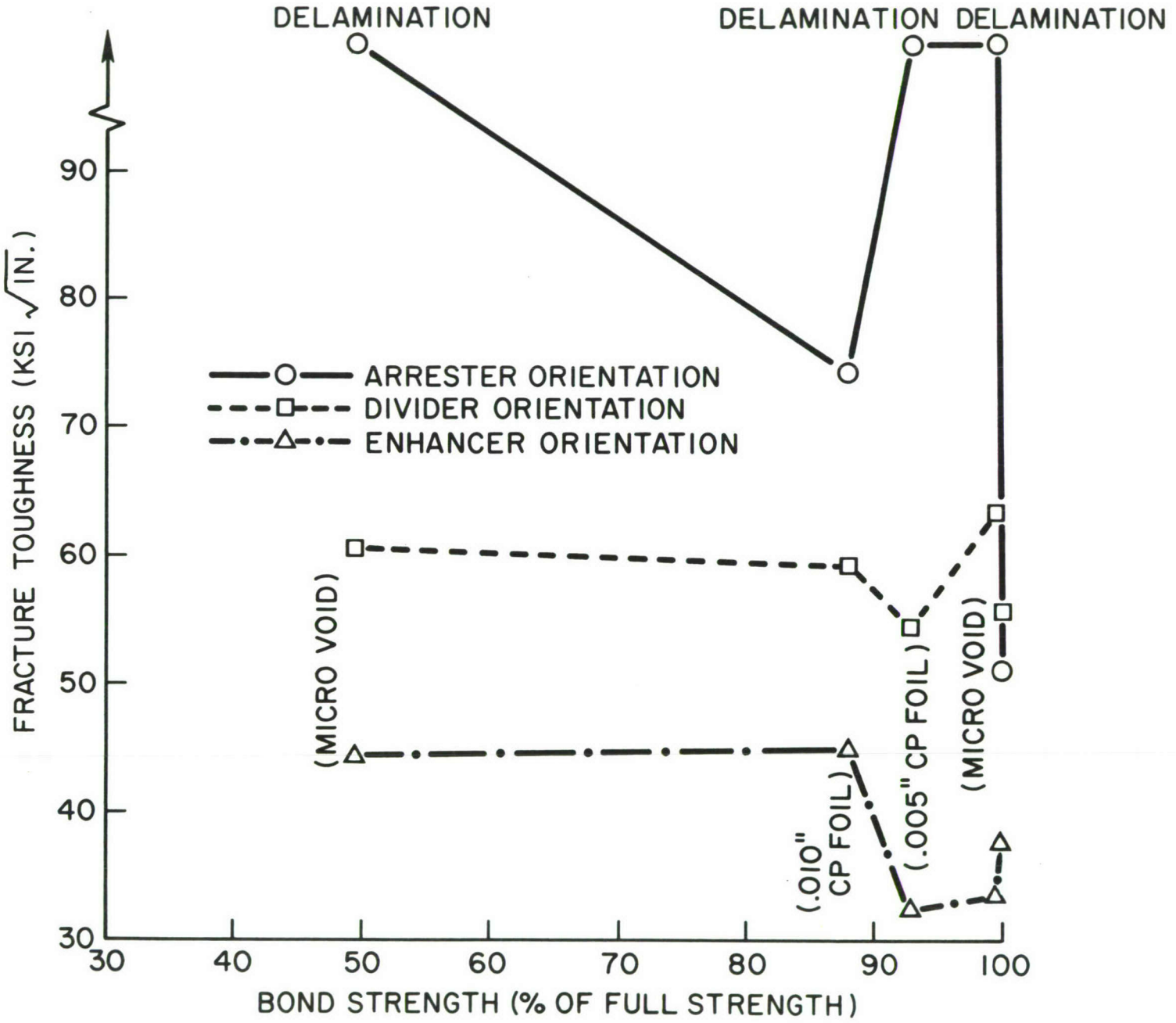

Figure 31. Fracture Toughness vs Relative Bond Strength for Material in the Heat Treated Condition

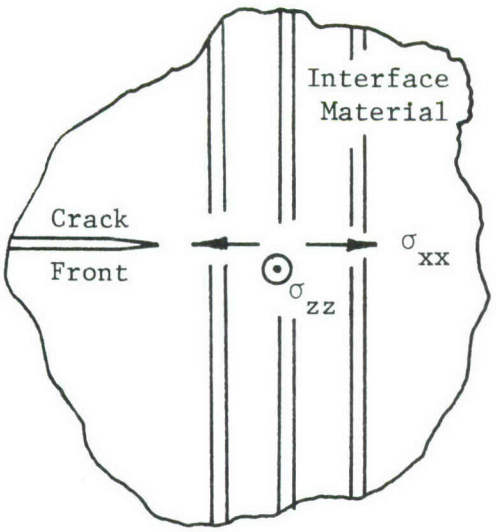

(a) Triaxial constraint produces transverse stresses

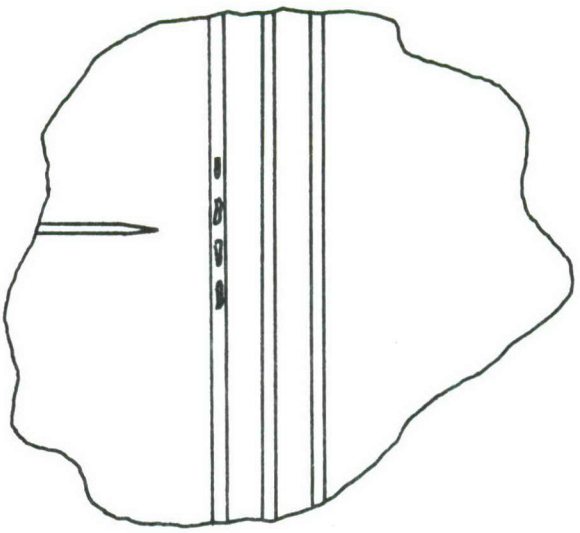

(b) Void formation in interface material

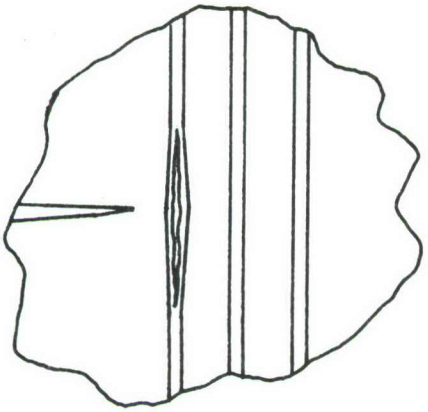

(c) Void growth and coalsence leading to delamination at the interface

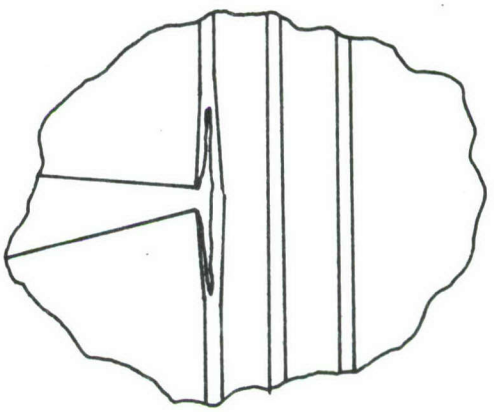

(d) Crack propagation to delamination and crack blunting

Figure 32 Steps that lead to delamination in the arrester orientation.

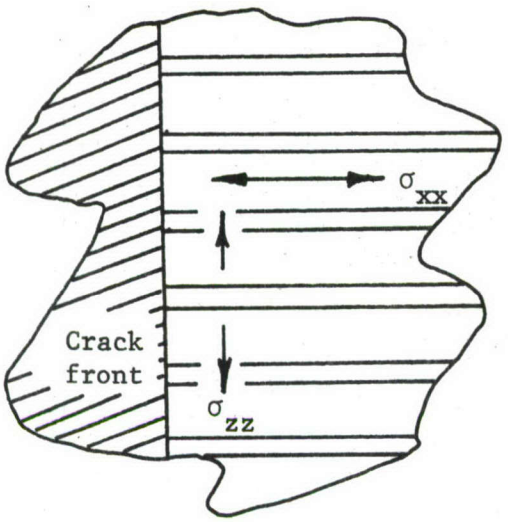

(a) Triaxial constraint produces transverse stresses

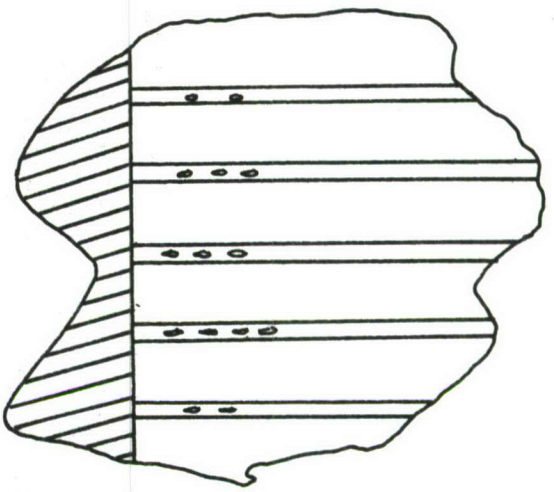

(b) Void formation in interface material

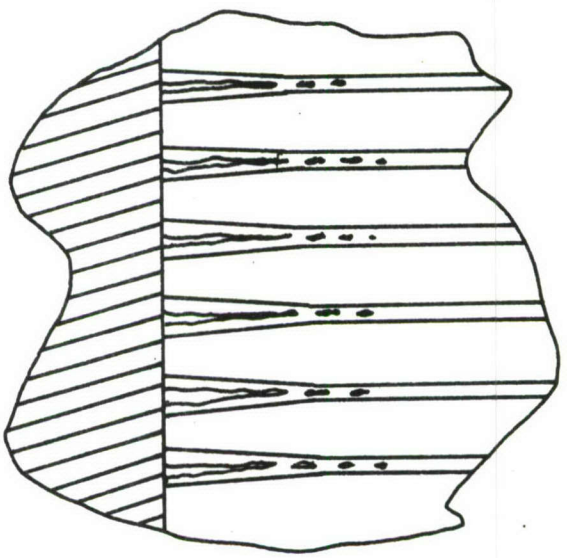

(c) Void growth and coalescence leading to delamination and splitting of material into thin sheets

Figure 33 Steps that lead to splitting in the divider orientation.

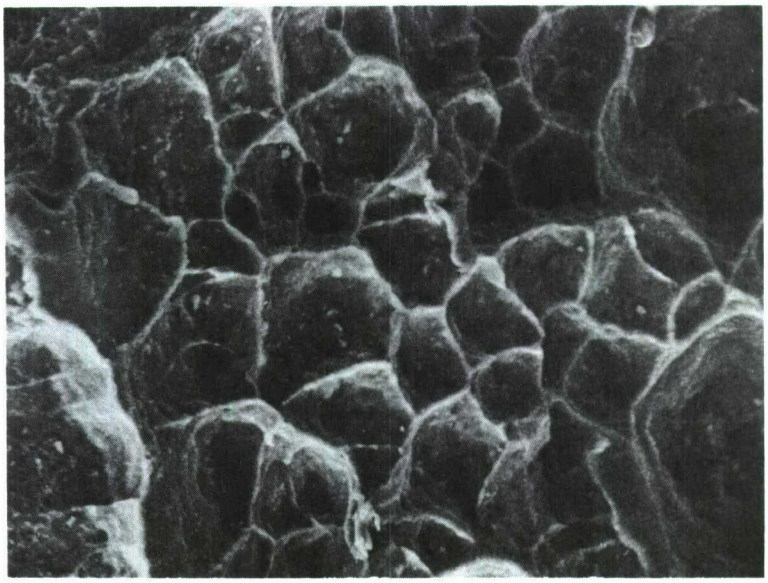

Figure 34 Fracture appearance of interface in divider orientation of Billet #6 (430X).

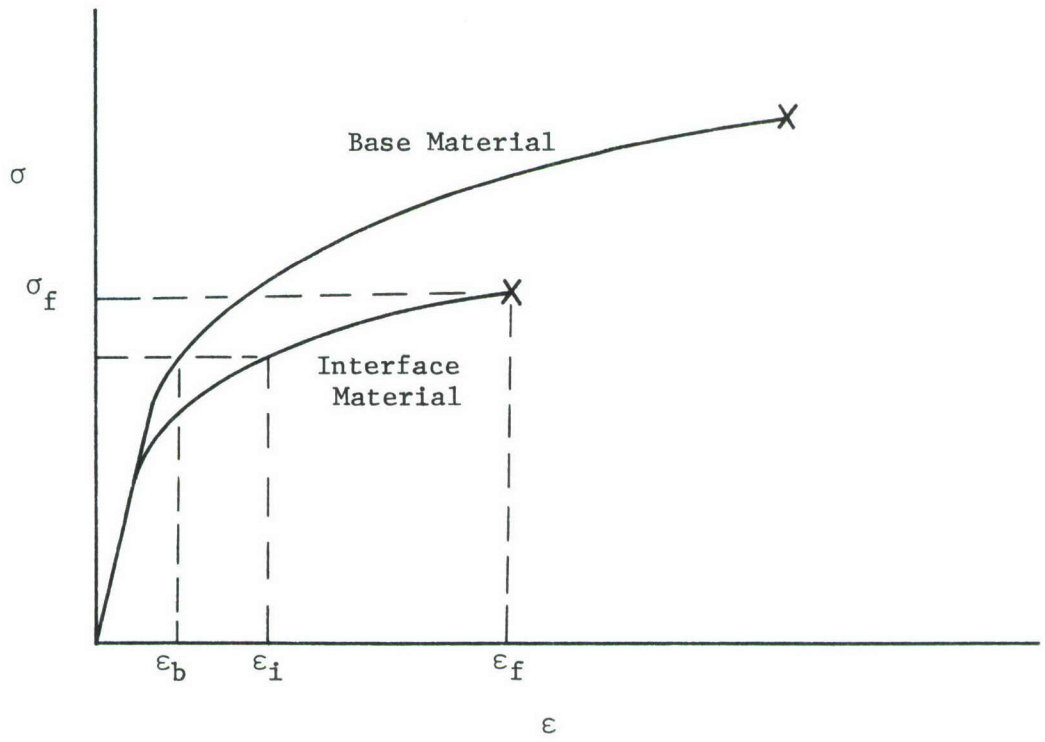

Figure 35 Schematic stress-strain curve for base and interface material.

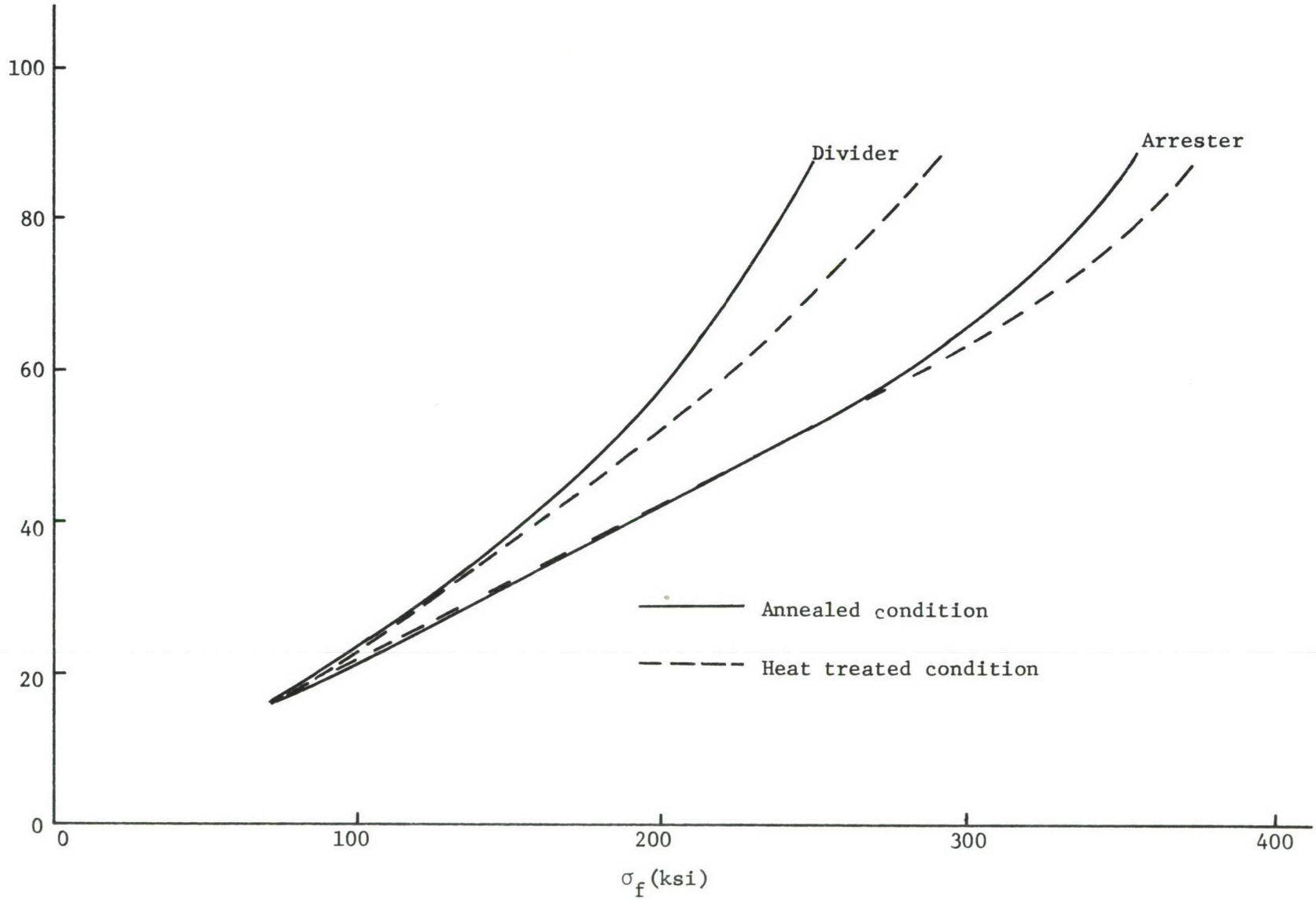

Figure 36 Critical stress intensity factor $(K_I)_s$ as a function of fracture stress σ_f.

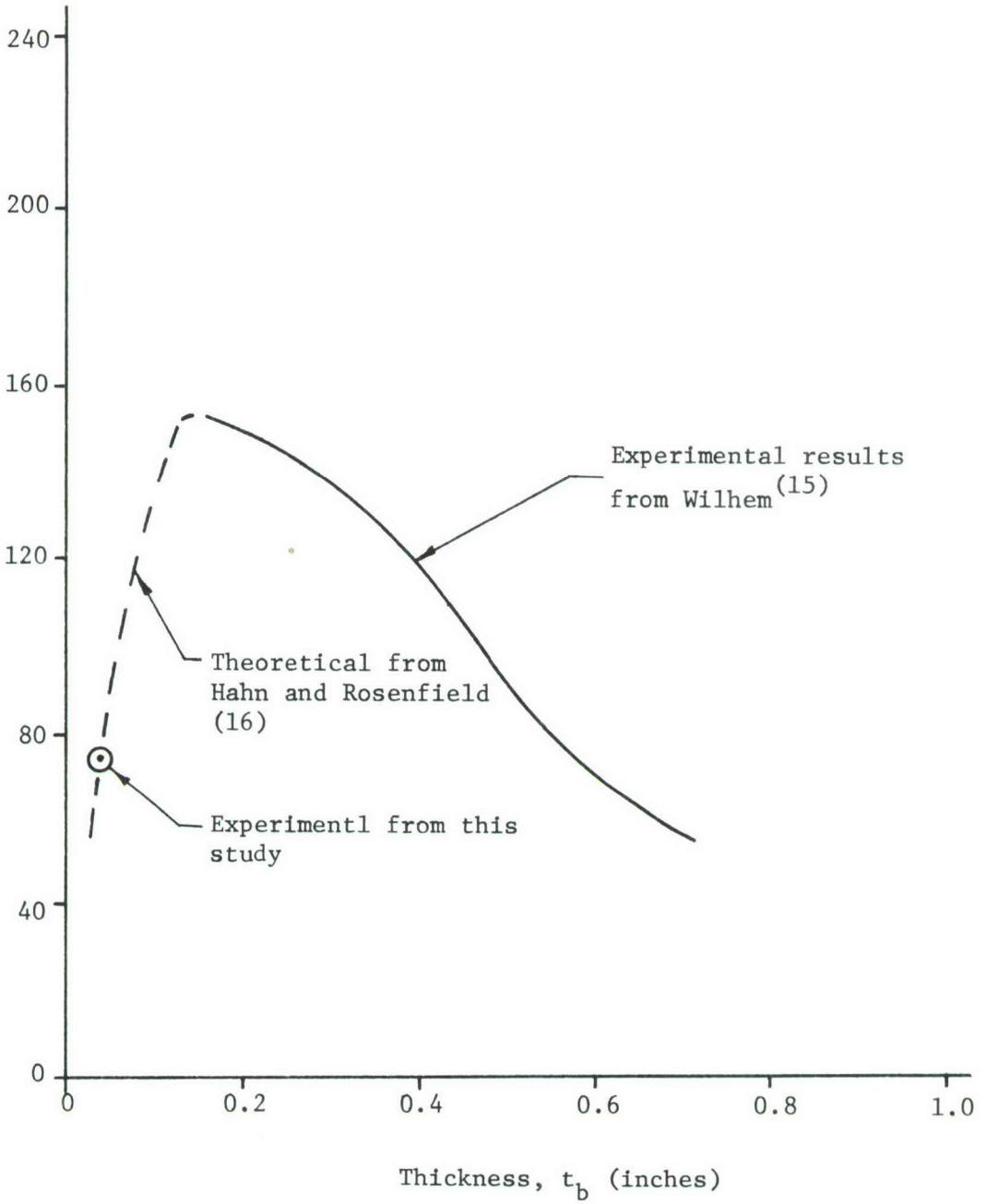

Figure 37 K_c vs. thickness for 6Al-4V titanium material.

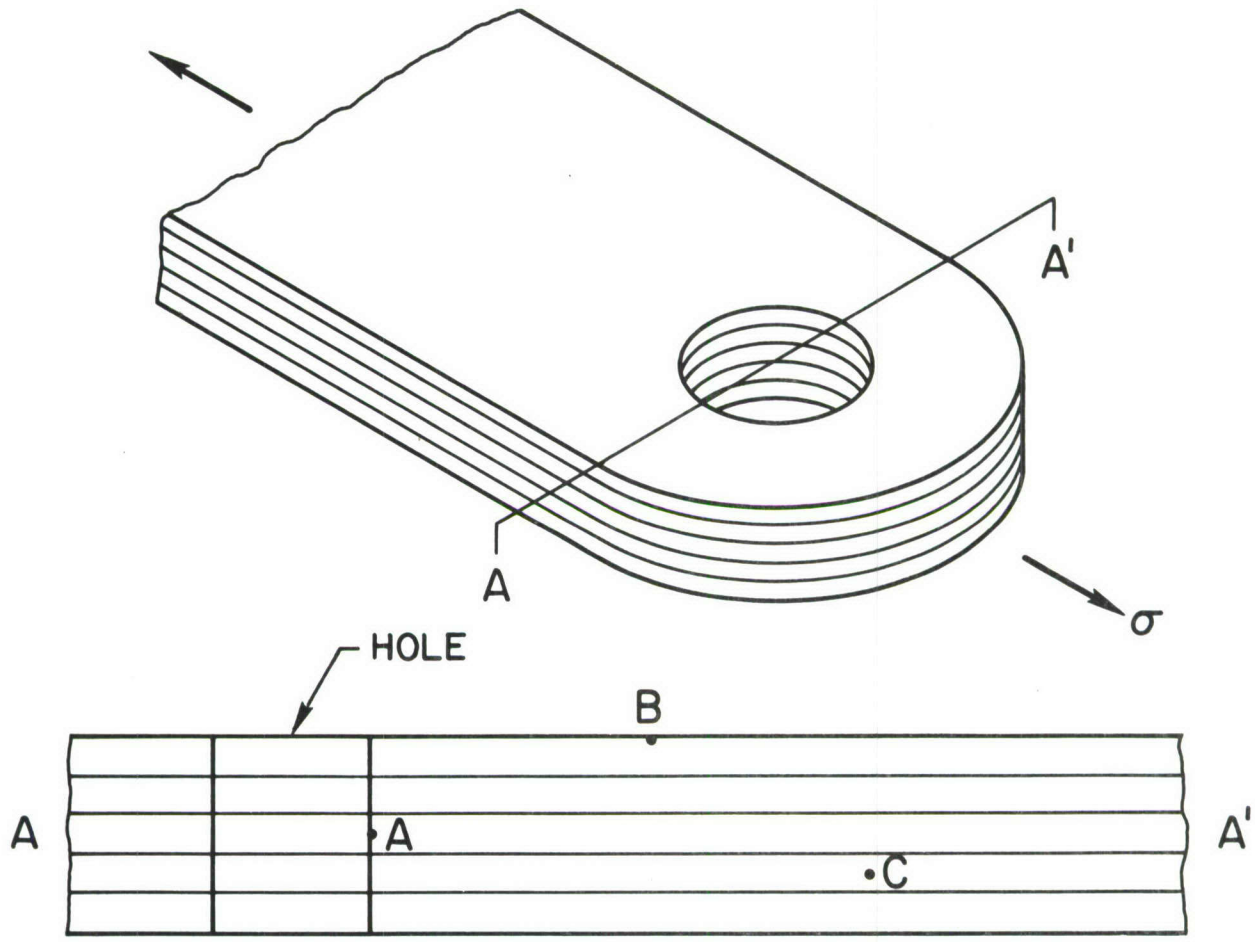

(a)

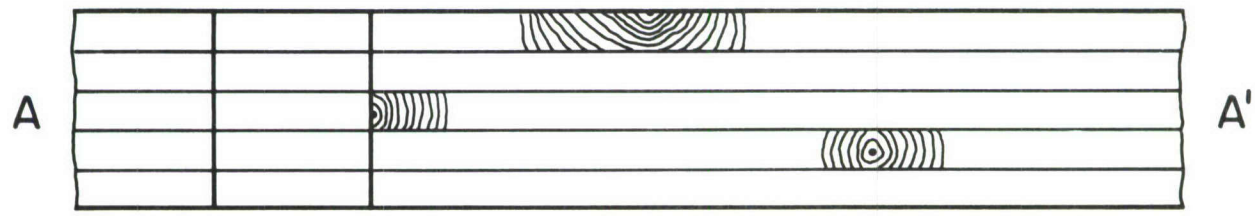

(b)

FIGURE 38. CRACK CHANNELING IN LAMINATE COMPOSITES

Security Classification

DOCUMENT CONTROL DATA - R & D

(Security classification of title, body of abstract and indexing annotation must be entered when the overall report is classified)

1. ORIGINATING ACTIVITY *(Corporate author)*
Failure Analysis Associates
P. O. Box 4227
Stanford, California 94305

2a. REPORT SECURITY CLASSIFICATION
Unclassified

2b. GROUP

3. REPORT TITLE
Improved Fracture Toughness of Ti-6Al-4V Through Controlled Diffusion Bonding

4. DESCRIPTIVE NOTES *(Type of report and inclusive dates)*
Final Report 1970, November through 1971, November

5. AUTHOR(S) *(First name, middle initial, last name)*
Donald O. Cox and Alan S. Tetelman

6. REPORT DATE	7a. TOTAL NO. OF PAGES	7b. NO. OF REFS
February 1972	81	16

8a. CONTRACT OR GRANT NO.	9a. ORIGINATOR'S REPORT NUMBER(S)
F 33615-71-C-1062	
b. PROJECT NO. 7381 =	5-829
c.	9b. OTHER REPORT NO(S) *(Any other numbers that may be assigned this report)*
d.	AFML-TR-71-264

10. DISTRIBUTION STATEMENT
This document has been approved for public release and sale; its distribution is unlimited.

11. SUPPLEMENTARY NOTES	12. SPONSORING MILITARY ACTIVITY
	Air Force Materials Laboratory Air Force Systems Command (45433) Wright-Patterson Air Force Base, Ohio

13. ABSTRACT

The use of laminate composites containing a weak interface to increase the fracture toughness of high strength titanium alloys has been studied. Billets were fabricated from .040 inch Ti-6Al-4V sheet material using a diffusion bonding process. Six billets were fabricated, each billet having an interface with different properties.

Weak interfaces were produced by incomplete diffusion bonding (two billets), by the use of a commercially pure titanium interleaf (two billets), or by the use of an unalloyed aluminum interleaf. One billet was fabricated with a full strength bond (no interleaf) for use as a control billet for comparison purposes.

Tensile tests on as-fabricated material were made to determine the interface bond strength. Fracture toughness tests were made using precracked Charpy specimens for material in both heat treated and annealed conditions. Three possible orientations of the crack to the interface were tested.

Results indicate that toughness, as measured by the precracked Charpy test, is increased when delamination or splitting of the bond occur. In the arrester orientation the toughness became very high as gross yielding occurred after delamination. In the divider orientation the fracture mode was changed from plane strain to plane stress when delamination occurred and the fracture toughness for the composite approached the toughness of the .040 inch sheet used in fabrication. Decreases in toughness occurred when the crack propagated along the bond plane. These results indicate that controlled diffusion bonding may offer promise for improving the

DD FORM 1 NOV 65 1473

Security Classification

Report # AFML-TR-71-264

Item 13. Abstract - continued

toughness in certain directions of orthotropic metal laminates without producing significant decreases in transverse strength or toughness.

A simple model to predict the conditions necessary for delamination has been formulated. Correlations between the model and experimental results are made. The model can account for the effect of different base metal and interface material properties and thicknesses. It is seen that a thin, low yield strength interface material with a full strength diffusion bond to a high yield strength, fairly tough base metal leads to optimum composite toughness.

14. KEY WORDS	LINK A		LINK B		LINK C	
	ROLE	WT	ROLE	WT	ROLE	WT
Titanium Alloy Ti-6Al-4V						
Laminate Composite						
Diffusion Bond						
Fracture Toughness						